

**EXPLORATION FOR BLIND GEOTHERMAL RESOURCES IN THE  
STATE OF HAWAI'I UTILIZING DISSOLVED NOBLE GASSES IN  
WELL WATERS**

A THESIS SUBMITTED TO THE GRADUATE DIVISION OF  
THE UNIVERSITY OF HAWAI'I AT MĀNOA IN PARTIAL FULFILLMENT  
OF THE REQUIREMENTS FOR THE DEGREE OF

MATER OF SCIENCE

IN

GEOLOGY AND GEOPHYSICS

NOVEMBER 2020

By

Colin M. Ferguson

Thesis Committee:

Scott Rowland, Chairperson

Nicole Lautze

Donald Thomas

Keywords: Geothermal, geochemistry, noble gases, Hawai'i

## Acknowledgements

First and foremost, I would like to thank my family, Mireya, Archer, and Griffin, for supporting me, for understanding this personal goal, for tolerating the time lost, and the expenses incurred. While this adventure is coming to an end, so many more now await us ahead.

I would like to thank the following persons and organizations for their help with well access and sampling: The Department of Water, County of Kaua'i, particularly Andy Canavan. Todd Presley of the USGS. Pūlama Lāna'i, especially Joy Gannon and Kevin Humphrey. The Department of Water Supply, County of Hawai'i, particularly Mae Kise. Rick Strojny of Pu'u Lani Ranch. Stephen Green and Kimber Deverse of Hawai'i Water Service. Diane Ford and Kanoa Alapai of Waiki'i Ranch. Kyle Teraoka of the US Department of the Navy Facilities Management. I would also like to thank the owners of private wells for allowing access. Without the people listed above, this project would have no data.

I would like to thank Professor Nicole Lautze, for offering me the opportunity to work on an exciting and meaningful project, and for trusting me to manage and complete it. I would like to thank my committee chair, Scott Rowland, for always being there when needed. I would like to thank my entire committee for their guidance, their patience, and their contributions to this work.

I would like to thank Professors Michael Garcia, Garret Ito, and John Sinton of the University of Hawai'i at Mānoa for their sharing of knowledge of Hawaiian geology. Doctor Burton Kennedy for his knowledge and contributions to noble gas geochemistry as it pertains to geothermal research, and the sharing of data. Professor Daniele Pinti of the University of Québec at Montréal, and Doctor Andrew Hunt of the United States Geologic Survey, for their scientific support and mentoring. Robert Whittier of the Hawai'i Department of Health for his knowledge of water chemistry and lithology on O'ahu. PhD candidate Diamond Tachera of the University of Hawai'i at Mānoa for establishing and maintaining working relationships with community members, through which many of my contacts were made, and for her prior work on the chemistry of well waters of Hawai'i. I thank Professor Davianna McGregor for her open conversations with me about Pele and Hawaiian Religion, and her assistance with the preface to this study.

I also thank the US Department of Energy for funding the Play Fairway Projects, and for fostering geothermal research through the Geothermal Technologies Office. Finally, I thank the Geothermal Resources Council (now Geothermal Rising) for championing geothermal energy, for being a supportive environment for geothermal research and innovation, and for providing a valuable location to exchange ideas and present research.

## Abstract

This study is an extension of the Hawaii Play Fairway Analysis (PFA), a statewide geothermal exploration project funded by the United States Department of Energy. Based on results from prior phases of the PFA, this project targeted 66 wells on the islands of Hawai‘i, Maui, Lāna‘i, O‘ahu, and Kaua‘i for sampling of dissolved noble gases, trace metals, common ions, and the stable isotopes  $^2\text{H}$  and  $^{18}\text{O}$ . Ultimately, 23 of the 66 well targets were sampled. Noble gas data from this study is supplemented with data shared by the United States Geologic Survey for the summit of Kīlauea, and by the geothermal energy company Ormat Technologies Inc. for their geothermal power plant Puna Geothermal Venture on the Lower East Rift of Kīlauea, and for their exploration of Kona and Hualālai on Hawai‘i, as well as the Southwest Rift of Haleakalā on Maui. The noble gas helium is used as an indicator of geothermal heat when excess  $^3\text{He}$  and/or  $^4\text{He}$  is present when compared to the atmospheric ratio of those isotopes ( $R/R_a$ ).  $R/R_a$  is minimally affected by dilution and transport, allowing even those wells not perfectly situated over a geothermal system to indicate a geothermal anomaly.  $R/R_a$  anomalies are present on every island in this study. There is a strong correlation between  $R/R_a$  anomalies and proximity to rift zones and calderas. Across the islands  $R/R_a$  ranged from 15-16 on Kīlauea’s lower east rift zone, which is a mantle plume value, to 0.37 on Lāna‘i, which is a crustal value. The majority of anomalous well samples had  $R/R_a$  values consistent with an upper mantle source. Mixing between upper mantle and crustal helium is evident on all islands. Geographically,  $R/R_a$  decreases from the high at Kīlauea to upper mantle values at Mauna Loa, and remains at upper mantle values for all wells across the other volcanoes, with the exception of two of four sampled wells on Lāna‘i, which have radiogenic, crustal  $R/R_a$  values ( $<1$ ). The trend of steeply decreasing  $R/R_a$  spatially, from plume-like to upper-mantle values, and then relatively constant values to Kaua‘i is consistent with fluid transport in the upper mantle in the direction of plate motion, and migration of noble gases into that fluid reservoir. Due to the association of helium with heat, it is likely that geothermal resources of undetermined potential are present on most Hawaiian Islands.

## Table of Contents

<b>Acknowledgements</b> .....	<a href="#"><u>ii</u></a>
<b>Abstract</b> .....	<a href="#"><u>iii</u></a>
<b>1. Introduction</b> .....	<a href="#"><u>1</u></a>
1.1. Purpose of Study .....	<a href="#"><u>1</u></a>
1.2. Noble Gases and Geothermal Resources .....	<a href="#"><u>1</u></a>
1.3. Geothermally Relevant Hydrology and Geology of the Hawaiian Islands .....	<a href="#"><u>5</u></a>
1.4. Previous Geothermal Assessments of the Hawaiian Islands .....	<a href="#"><u>8</u></a>
<b>2. Methods</b> .....	<a href="#"><u>10</u></a>
2.1. Site Selection.....	<a href="#"><u>10</u></a>
2.2. Explanation of Prospecting Parameters Used .....	<a href="#"><u>11</u></a>
2.3. Sample Collection and Analysis .....	<a href="#"><u>18</u></a>
2.4. Equations .....	<a href="#"><u>20</u></a>
<b>3. Results</b> .....	<a href="#"><u>24</u></a>
3.1. Statewide Overview.....	<a href="#"><u>24</u></a>
3.2. Model Results .....	<a href="#"><u>26</u></a>
3.3. Kaua‘i .....	<a href="#"><u>30</u></a>
3.4. O‘ahu .....	<a href="#"><u>30</u></a>
3.5. Lāna‘i.....	<a href="#"><u>31</u></a>
3.6. Maui.....	<a href="#"><u>31</u></a>
3.7. Hawai‘i .....	<a href="#"><u>31</u></a>
3.7.1. Kīlauea .....	<a href="#"><u>31</u></a>
3.7.2. Mauna Loa .....	<a href="#"><u>32</u></a>
3.7.3. Hualālai.....	<a href="#"><u>32</u></a>
3.7.4. Waikoloa .....	<a href="#"><u>32</u></a>
<b>4. Discussion</b> .....	<a href="#"><u>33</u></a>
4.1. Statewide Overview.....	<a href="#"><u>33</u></a>
4.1.1. Kaua‘i.....	<a href="#"><u>38</u></a>
4.1.2. O‘ahu .....	<a href="#"><u>40</u></a>

4.1.3. Lāna‘i.....	<a href="#">43</a>
4.1.4. Maui – Haleakalā.....	<a href="#">44</a>
4.1.5. Hawai‘i - Hualālai and Waikoloa .....	<a href="#">45</a>
4.1.6. Hawai‘i - Kīlauea and Mauna Loa .....	<a href="#">47</a>
4.2. Mantle Helium Trends Along the Main Hawaiian Chain.....	<a href="#">50</a>
<b>5. Conclusions.....</b>	<a href="#">52</a>
<b>References.....</b>	<a href="#">53</a>

### List of Tables

Table 1. Well Sampling Criteria .....	<a href="#">15</a>
Table 2. Stable Isotopes $\delta^{18}\text{O}$ and $\delta\text{D}$ .....	<a href="#">25</a>
Table 3. $\text{R}/\text{R}_a$ from Tritiogenic $^3\text{He}$ .....	<a href="#">27</a>
Table 4. $\text{R}/\text{R}_a$ from Radiogenic $^4\text{He}$ .....	<a href="#">28</a>
Table 5. Helium Values $\text{R}/\text{R}_a$ , $\text{R}_c/\text{R}_a$ , and $\text{F}(^4\text{He})$ .....	<a href="#">29</a>

### List of Figures

Figure 1. $\text{R}/\text{R}_a$ for North American Geothermal Systems .....	<a href="#">3</a>
Figure 2. $\text{R}/\text{R}_a$ for Global Volcanic Systems .....	<a href="#">5</a>
Figure 3. Map of the Main Hawaiian Chain and associated Volcanoes .....	<a href="#">6</a>
Figure 4. Conceptual Rift or Caldera Hosted Geothermal System.....	<a href="#">7</a>
Figure 5. Map of Play Fairway Areas of Interest and Well Targets in this study .....	<a href="#">16</a>
Figure 6. $\text{Cl}/\text{Mg}$ vs Well Temperature Plot .....	<a href="#">17</a>
Figure 7. Filled and Sealed Sample Tubes .....	<a href="#">19</a>
Figure 8. Plot of $[\text{He}]$ vs $\text{R}/\text{R}_a$ .....	<a href="#">34</a>
Figure 9. Meteoric Water Line for $\delta^{18}\text{O}$ and $\delta\text{D}$ .....	<a href="#">35</a>
Figure 10. $\text{F}(^4\text{He})$ vs $\text{R}/\text{R}_a$ Mixing Lines.....	<a href="#">37</a>
Figure 11. Inset of Figure 10 for Low $\text{R}/\text{R}_a$ and $\text{F}(^4\text{He})$ Values .....	<a href="#">38</a>
Figure 12. Map of Kaua‘i Samples and their Helium Values .....	<a href="#">39</a>
Figure 13. Map of O‘ahu Samples and their Helium Values .....	<a href="#">41</a>

Figure 14. Microphoto of Alteration Minerals from O‘ahu .....	<a href="#">42</a>
Figure 15. Map of Lāna‘i Samples and their Helium Values .....	<a href="#">43</a>
Figure 16. Map of Haleakalā Samples and their Helium Values .....	<a href="#">44</a>
Figure 17. Map of Hualālai and Waikoloa Area Samples and their Helium Values .....	<a href="#">46</a>
Figure 18. Map of Mauna Loa Samples and their Helium Values .....	<a href="#">48</a>
Figure 19. Map of Kīlauea Samples and their Helium Values .....	<a href="#">49</a>
Figure 20. Conceptualized Cross Section of Main Hawaiian Chain and R/R <sub>a</sub> Trends .....	<a href="#">51</a>

## Preface

The Hawaiian akua, Pele, the elemental of magma and lava and all manifestations of the volcanic life force, including steam, resides within the Kīlauea Volcano, centered at Halema‘uma‘u, the crater atop Kīlauea. Pele is relevant to geothermal studies in Hawai‘i. Chants document the pattern of volcanic eruptions associated with the life force of Pele, as the Hawaiian Islands dwelled over the hot spot. The eruptions are documented as a story of Pele’s journey across the Pacific, and lingering at every Hawaiian island, creating new land. Finally, it is at Halema‘uma‘u that the volcanic life force settles as she found a suitable location. From there she brings creation of new land and replenishment of old land.

The Pele life force is not alone, as there are many other akua, some of which work together, others against each other. Combined, the akua are not just deities, but actual manifestations of all of the phenomena associated with the natural world. The journey of Pele reflects the travels of the Hawaiian people, and their knowledge about the formation of the Hawaiian Islands. The order in which Pele stopped along the Hawaiian Islands matches their geologic age, and indeed, the Hawaiians were aware of these relative age relationships and volcanic origin. Where Pele lingered on the older islands, there are rejuvenation volcanics. Exemplifying this are a number of mele, chants, that overlap with historic eruptions of Kīlauea and elsewhere. The explosive eruptions of the late 1700’s are tied to a mele describing a quarrel where Pele threw stones at Kamapua‘a, a fertility akua, who had a volatile relationship with Pele.

Traditional Hawaiian religion, continuously practiced since the settling of the islands, serves as a means of passing on important and practical scientific information, that connected people to the land, their ancestors, and history. The Hawaiian families residing on Kīlauea in the district of Puna on the Island of Hawai‘i were, and some still are, very connected to Pele. Their love and stewardship of the land is represented in that relationship. To them, and many other Native Hawaiians, much of Kīlauea is kapu, sacred, out of respect for Pele. This also has practical meaning, in acknowledging the risks and dangers associated with active volcanism. Offerings and prayers are made to enter her lands to this day, to ensure successful outings.

While one need not believe in Pele, when working in Hawai‘i it is important to acknowledge the living presence of the akua in the minds of many. Being respectful as one would in any sacred site, such as a church, is a best practice. This can have limits on what we as scientists are able to freely do, but often there is a way to work within those bounds. Embedding the local community in our work will always have mutual benefits for all involved. Thinking forward about how those local communities might benefit or be harmed by any results is absolutely our responsibility, and we should always design our projects in the most equitable, inclusive, and ethical way when considering the local communities.

## **1. Introduction**

### **1.1 Purpose of Study**

This study is a component of the Hawai'i Play Fairway Project (PFA), which is a statewide assessment for potential geothermal resources funded by the United States Department of Energy (DE-FOA-0000841). The Play Fairway technique involves identifying the geologic characteristics (e.g. structure, chemistry, age, etc.) that indicate the presence of a subsurface resource (ore, geothermal, oil) over an area of interest, or Fairway, then compiling or obtaining such data, and finally integrating such data into a map of resource probability. The Hawai'i Play Fairway Project (PFA) defined the State of Hawai'i as its Fairway, and identified 10 Plays (Lautze et al, 2017b). The total project incorporated multiple types of geological, geophysical, and groundwater data. This study is focused specifically on dissolved noble gas data as sampled in well waters across the state.

The Hawaiian Islands are primarily dependent on imported fossil fuels for the generation of electricity. This leaves Hawai'i with a large carbon footprint, vulnerable to disruptions in global supply, and paying the highest electric utility costs in the United States (EIA 2020). With a state mandate to achieve carbon neutrality and 100% renewable energy by 2045, exploration for, and characterization of, any unknown geothermal reservoirs is key to knowing what renewable energy options are available. In this study, I used dissolved noble gases (primarily helium) to explore for thermal influences within Hawaiian groundwater at selected wells statewide. In addition to helium, argon and neon were used as complimentary elements and for standardization. The goal was to identify any potential blind (i.e., without surface expression) geothermal systems for additional investigation.

### **1.2 Noble Gases and Geothermal Resources**

The noble gases are chemically inert, highly volatile elements. Because of these characteristics, they will only fractionate through physical processes (i.e. boiling, dissolution). When dissolved in magma or water the majority of noble gases present will stay dissolved until they are stripped out by the formation of bubbles of other volatiles (i.e. CO<sub>2</sub>), or through diffusion to the atmosphere. The small fraction of noble gases trapped in fluid inclusions and defects in a

mineral's crystal lattice can be released when the mineral is heated. As such, the noble gases make excellent tracers for a number of geologic and hydrologic processes. The most important noble gas for geothermal exploration is helium due to it being less sensitive to dilution, and its association with heat.

The relationship between helium and geothermal heat has been known for decades (e.g. Torgersen and Jenkins 1982, Welhan et al. 1988). Groundwater will interact with a heat source from an increased geothermal gradient through crustal thinning, or from rising magma, and in the process take up available noble gases (and also heat). Generally, for geothermal research one can measure the dissolved noble gases on Earth's surface at hot springs and in wells, and as gases in fumaroles. Due to the rarity of geothermal surface features in Hawai'i, exploration away from active surface volcanism must rely on wells alone.

To analyze sources of helium, I use the dissolved concentration (cc/g – volume of gas in cubic centimeters per gram of solution, in this case water) of helium isotopes,  $^3\text{He}$  and  $^4\text{He}$ . The majority of  $^3\text{He}$  is primordial, inherited from the formation of the Earth. However, some is produced from thermal neutron capture by lithium (Ballentine and Burnard 2002), as well as through cosmogenic production of tritium ( $^3\text{H}$ ) in the atmosphere, which decays to  $^3\text{He}$ . These are both important processes in the near surface but they do not substantially influence geothermal systems. Within the Earth  $^4\text{He}$  is almost entirely radiogenic, formed from the decay of uranium ( $^{235}\text{U}$  and  $^{238}\text{U}$ ) and thorium ( $^{232}\text{Th}$ ) (Ballentine and Burnard 2002).

For this study, I used the standard helium isotope ratio  $R/R_a$ , where  $R$  is the ratio of  $^3\text{He}/^4\text{He}$  in a sample, and  $R_a$  is the atmospheric ratio of these same isotopes ( $1.39 \times 10^{-6}$ ).  $R/R_a$  of the atmosphere is therefore 1.  $R/R_a$  of air saturated water (ASW) at  $20^\circ\text{C}$  and 1 atmosphere is 0.98, which is the result of small fractionation effects from dissolution. ASW values are equilibrium values between the atmosphere and surface water, and are dependent on temperature and pressure. The  $R/R_a$  of the upper mantle ranges from 6.5 to 9.5 (with a mean value of 8; Graham 2002). Crustal  $R/R_a$  varies by age and composition, but can have  $R/R_a$  similar to the ASW down to an  $R/R_a$  of 0.01 from the presence of radiogenically produced  $^4\text{He}$ .  $R/R_a$  values of waters from magmatically hosted geothermal systems (most of which are subduction related) are between those of ASW and the upper mantle, due to the mixing of the magmatically sourced helium with

that of the crust. In geothermal systems where there is no volcanism and only an enhanced geothermal gradient is present (a hot thinning lithosphere such as in the Basin and Range Province of the North American Plate), the radiogenic  $^4\text{He}$  released from rocks is in excess of ASW, and leads to  $R/R_a$  values as low as 0.01 (Figure 1). Mantle plumes, such as that which has produced the Hawaiian volcanoes, are very enriched in  $^3\text{He}$  compared to the upper mantle (Sedwick et al. 1994, Ozima and Podosek 2004, Graham et al. 2009, Harðardóttir et.al 2018, table 6.2 ). At Lō‘ihi seamount, the youngest Hawaiian volcano, the highest  $R/R_a$  measured is 35 (Valbracht et al. 1997). A compilation of some noble gas reservoirs is shown in Figure 2, and a compilation of  $R/R_a$  values for a number of plume and upper mantle sites is given in Jackson et al. (2017).

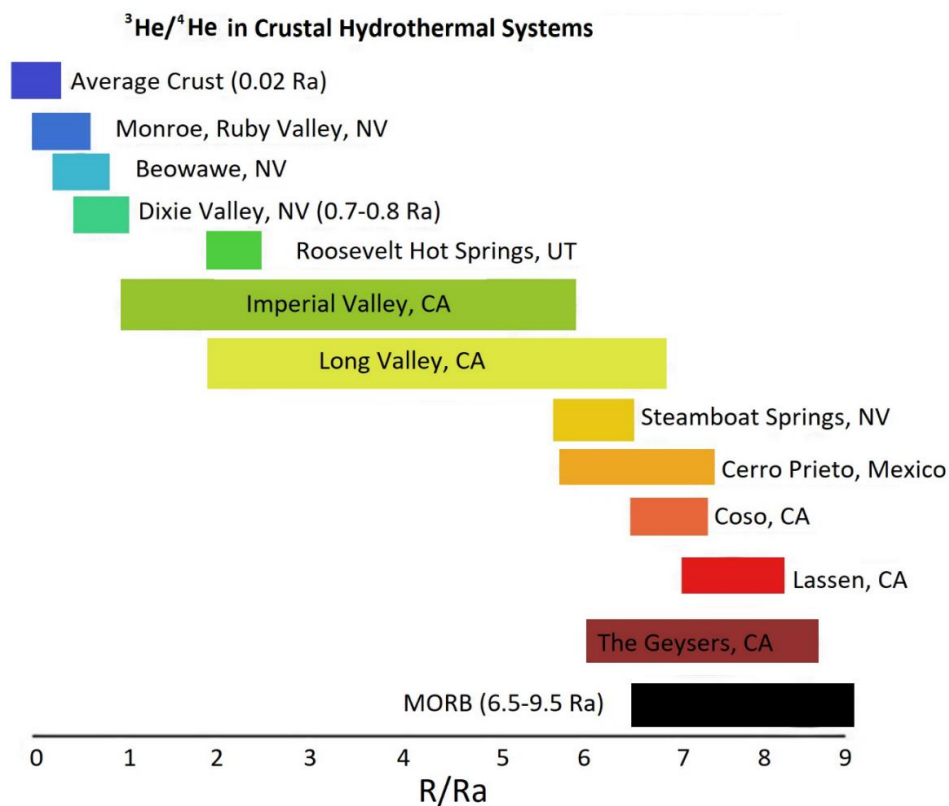


Figure 1. A compilation of  $R/R_a$  values for geothermal systems on the North American continent. Notice that these examples in total cover the full range of  $R/R_a$  values from crustal at  $<1$ , to that of the upper mantle  $\approx 8$ . None of these sites are plume related. Modified from Kennedy and Van Soest 2006.

It is worth noting that all geothermally related dissolved noble gases are diluted from their source values by groundwater. Continued dilution during transport leads to values progressively closer to the  $R/R_a$  of localized ASW. Diluted geothermal waters can lead to uncertainty about the identity of the heat source reservoir, how far a sample has traveled from that heat source, or in the case of total dilution (to an ASW  $R/R_a$ ), whether a heat source is present at all. In this study, it is also worth noting that I am not attempting to use noble gases as a geothermometer, and the exact location and depth of a resource cannot be ascertained from helium. Finally, the absence of an  $R/R_a$  anomaly does not mean there are no geothermal systems in an area, because it is possible for groundwater to be isolated from a geothermal source by volcanic structures or impermeable rocks or soils.

Where  $R/R_a$  anomalies in groundwater are present, a heat source must be nearby. In the case of Hawaiian Islands, it is likely heat is associated with magmatic intrusions, and not from a thinning crust, so while some helium would be coming from rocks near an intrusion, most of the helium will be coming from the heat source. Without heat present, the low volume of helium in rocks eliminates them as a possible source of helium in groundwater at ambient near-surface temperatures. At elevated temperatures helium can diffuse from rocks and minerals, and, depending on water/rock ratio and residence time, this diffusion can have an impact on the  $R/R_a$  values independently from that of the heat source itself. For example, making the unreasonable assumption of instantaneous exchange between water and rock, and subsequent instant removal without dilution of this water to where it could be sampled, it would take a water:rock (volume) ratio of 1:10 to 1:50 to bring an ASW water with  $R/R_a$  of 0.98 to an  $R/R_a$  of 8 when interacting with an average rock from the oceanic crust. While these water:rock ratios are not impossible, the assumptions made here leave uncertainties beyond scientific use, and are for illustrative purposes only.

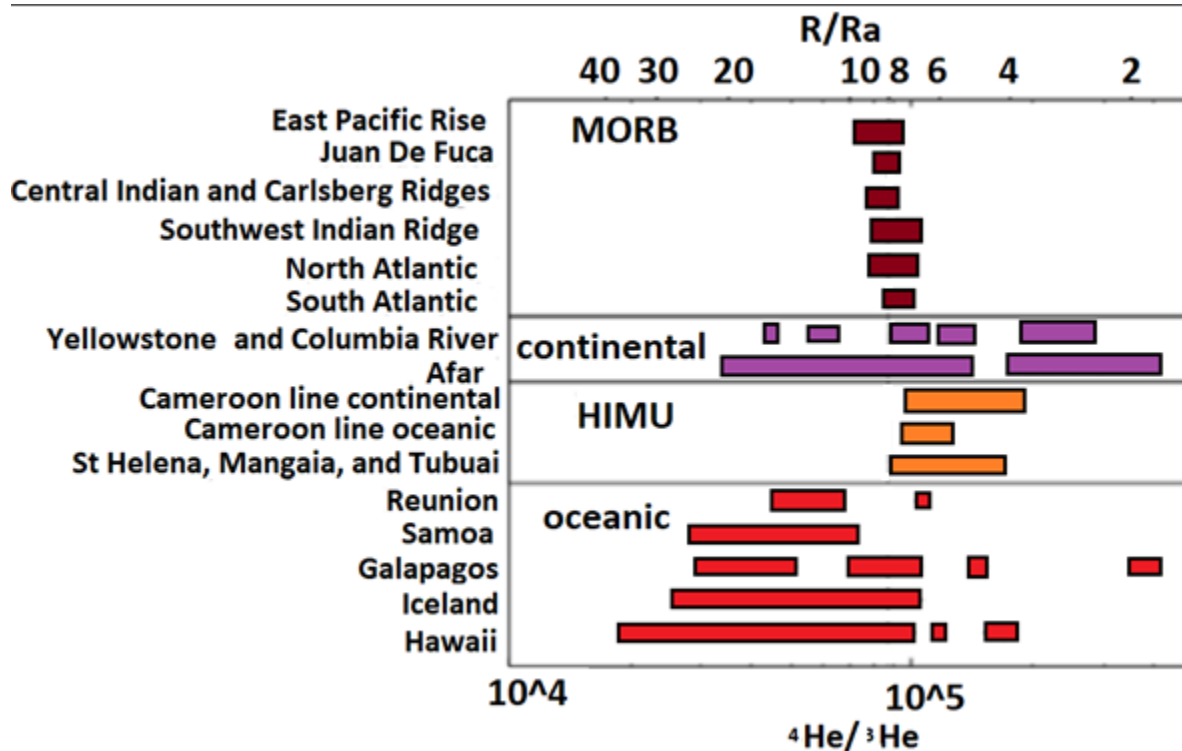


Figure 2. A selection of noble gas reservoirs, divided into mid-ocean ridge basalt (MORB), used here as “upper mantle”, plumes passing through continents, high  $^{238}\text{U}/^{204}\text{Pb}$  mantle (HIMU), and oceanic plumes. Vertical line at  $R/R_a$  8 represents the mean MORB value, which is the same value as the upper mantle. Modified from Barfod et al. 1999.

### 1.3 Geothermally Relevant Hydrology and Geology of the Hawaiian Islands

The Hawaiian Islands (Figure 3) are formed from mantle plume volcanism, producing primarily tholeiitic basalts. Eruptions are most common along rift zones and from caldera complexes, with rare eruptions elsewhere on volcano flanks (e.g., Macdonald et al. 1983). The plume is estimated to have a core temperature of at least 1550°C while within the mantle (Watson and Mackenzie 1991, Sisson 2003, Tree 2016.). At present, Kīlauea typically erupts at temperatures of 1140°C to 1200°C, but has been measured as high as 1250°C within lava tubes (Carling et al. 2015). At the surface, Hawaiian lava cools at variable rates, from 0.38 to 15°C/min (Flynn and Mougini-Mark 1992, Cashman et al. 1999). In the subsurface where groundwater may absorb long-term heat from a cooling magma chamber, magma may take thousands to millions of years to fully cool, depending on the depth and size of the magma chamber, and whether or not magma recharge from the plume is occurring (Annen and Sparks 2002, Coogan et al. 2007).

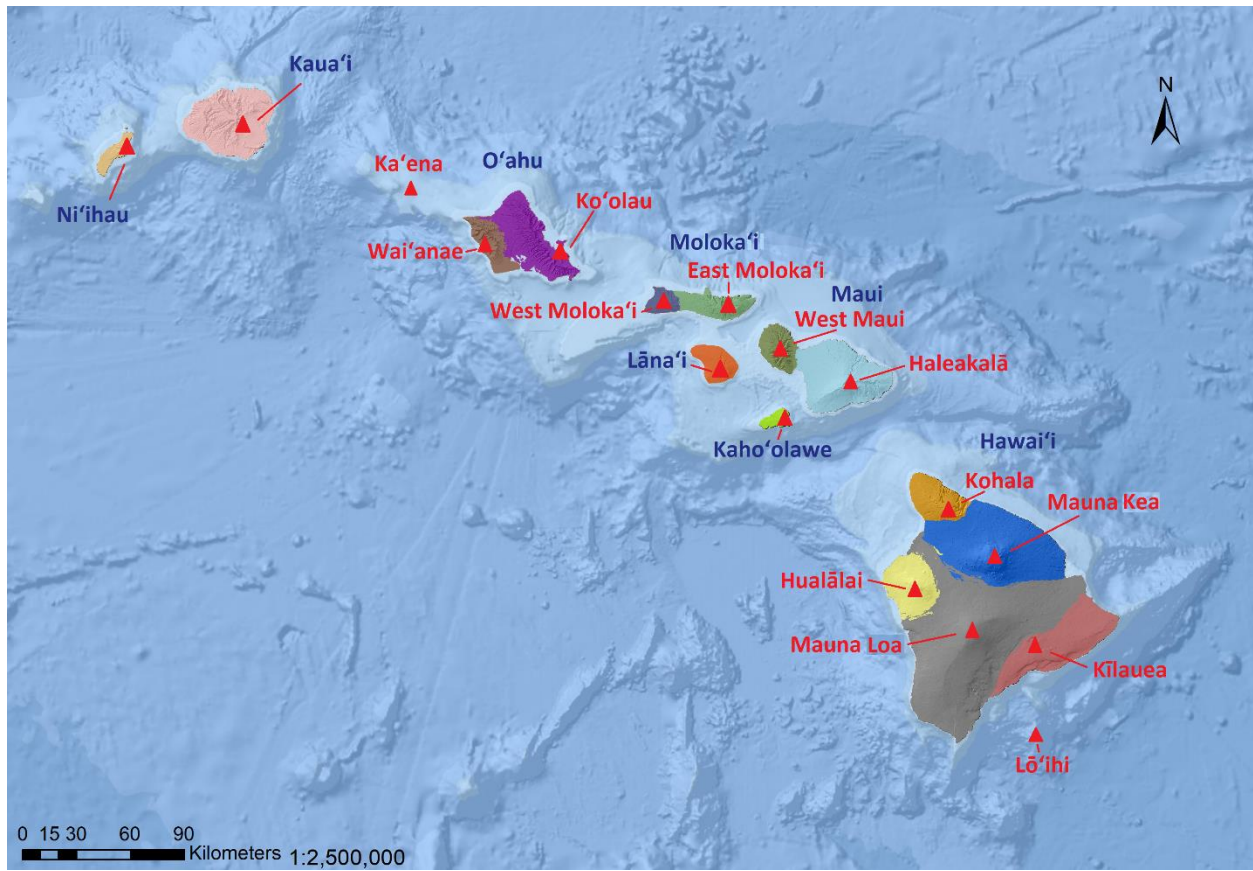


Figure 3. The Hawaiian Islands (names in blue) and their volcanoes (names in red).

The high porosity and permeability of basalts exposed at the surface allows meteoric water to rapidly recharge the basal aquifer, which subsequently forms a Ghyben-Herzberg lens (e.g., Macdonald et al. 1983). Groundwater flow and presence, including the freshwater lens, may be variable as groundwater flow paths within the Hawaiian Islands are controlled by lava flows, tephra, and dikes, allowing for discontinuity in groundwater flow and presence. Near vertical dikes can prevent groundwater flow in the horizontal direction, and compartmentalize groundwater, creating dike-impounded reservoirs. Lava flows may allow rapid horizontal flow. Tephra can reduce groundwater flow, and tuff deposits are impermeable when not highly fractured. Tropical soils and paleosols reduce recharge at the surface, and slow vertical permeability when buried under lava flows, which can form confined aquifers. Groundwater age across the islands is typically young. Water in West Hawaii was found to be between 35 and 70 years old (Kelly and Glen 2015). Isolated pockets of water within the island of Hawai'i have

been dated to approximately 7000 years (Thomas et al. 1996). The relatively high groundwater flow rate, cold freshwater lens, and geologic controls on vertical and horizontal flow may easily mask indications of the presence of geothermal resources (Figure 4).

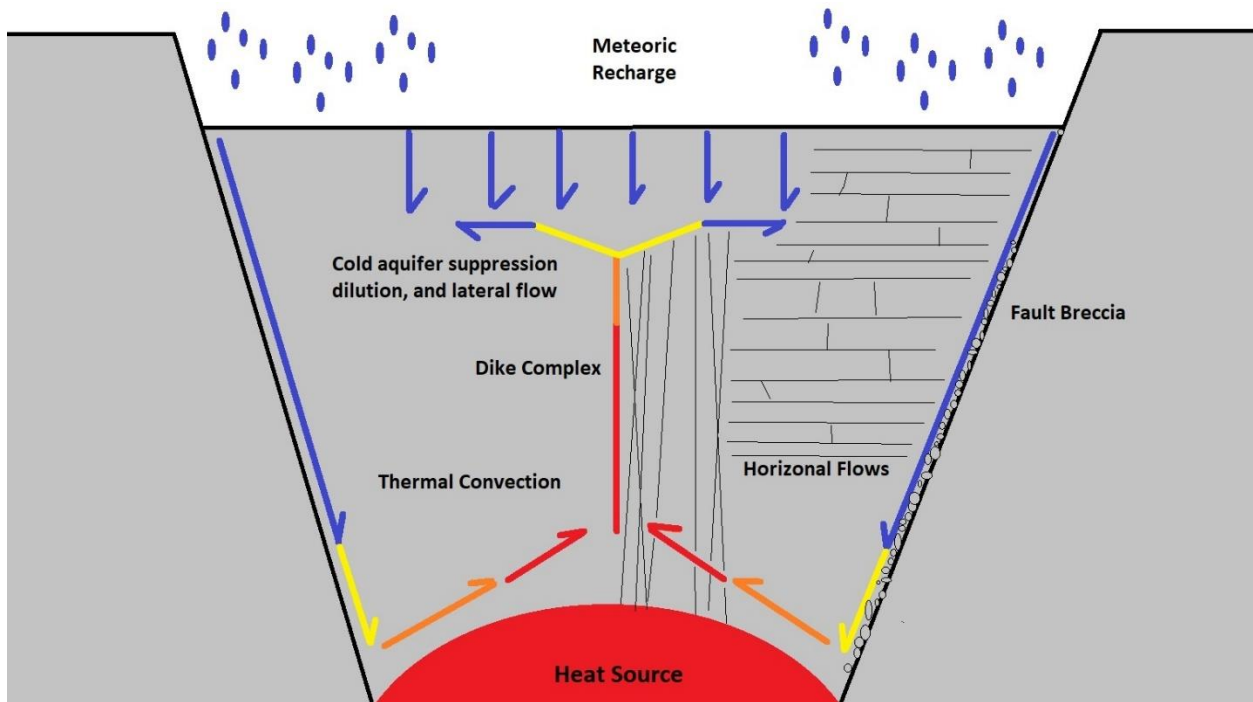


Figure 4. A thermal convective cell hosted in a caldera. Cold meteoric water will infiltrate the ground wherever possible, and move further into the subsurface along pathways such as faults where permeability can be high. Rising hot water moving towards the surface will draw in the cold recharge waters behind it, which in turn heat up, setting up the convective cell. The hot water will cool as it moves away from the heat source, in this case following a dike complex towards the surface until able to flow laterally, or until it is no longer thermally buoyant. Suppression of surface geothermal features is possible through horizontal lava flows, alteration filled fractures, and a cold water head above the heat source preventing the hot waters from fully reaching the surface.

## 1.4 Previous Geothermal Assessments of the Hawaiian Islands

Native Hawaiians, Kānaka Maoli, were the first to use geothermal energy in Hawai‘i. Along the east rift of Kīlauea (KERZ), hot rocks and steam vents were present, and warm waters discharge along the coast. These sites were used for cooking, heating, and bathing (Ellis 1827). Whereas early Westerners surely noticed these features, no investigation of them began until the 1960s.

In 1961, four exploratory holes were drilled into the KERZ in the Puna area by Hawai‘i Thermal Power Company and Magma Power Company. Although these holes encountered hot water, they were not determined to be of commercial value (Thomas et al. 1985). The next geothermal project was in 1972, and focused in the same area, Puna. Led by the University of Hawai‘i, the HGP-A well was drilled from 1975 to 76, and found 358°C waters at a depth of 1.97 km, with a flow of approximately 45 kL/hr (Thomas 1982). The HGP-A well powered a 2.8 MW power plant until 1989. That same year Ormat Technologies leased land in the Puna area near HGP-A, which is the site today of the only active geothermal power plant in Hawai‘i, the Puna Geothermal Venture (PGV).

A statewide assessment of geothermal resources began in 1978, and found 20 areas to target for additional exploration (Thomas et al. 1979). A second phase of exploration of those 20 areas was completed in 1985, and characterized 12 of the locations as having geothermal potential (Thomas 1985). The results show a strong relationship between geothermal potential and the youth of a volcano, decreasing with age and distance from the present position of the plume front (Lō‘ihi). The islands of Kaua‘i and Lāna‘i were not studied in the second phase project. Two statewide assessments were completed by GeothermEx under the direction of The State of Hawai‘i Department of Business, Economic Development, and Tourism (Geothermex 2000, Geothermex 2005). The 2000 and 2005 assessments found similar areas of interest to those of 1985, with the addition of potential resources on Moloka‘i and Lāna‘i. The Hawai‘i Statewide Play Fairway Analysis (PFA), funded by the U.S. Department of Energy Geothermal Technologies Office and undertaken by the University of Hawai‘i at Mānoa, is the first statewide assessment since 2005. Work on the PFA began in 2015, and this study is a continuation of the PFA research. The first phase of the PFA project identified geothermally relevant data, and compiled legacy data related to, or capable of, identifying heat, the presence of fluid, and permeability (Lautze et al. 2017a). From the compiled data, a statistical model for geothermal probability was developed (Ito et al.

2017), and applied to locate areas of interest for additional investigation (Lautze et al. 2017b). These areas of interest were studied through the collection of new geochemical and geophysical data, and an updated resource probability map has recently been produced (Lautze et al. 2020).

## 2. Methods

### 2.1 Site Selection

To select wells for sampling, I reviewed the results from the initial phases of the Hawai'i PFA project, which identified areas of relatively high probability of geothermal resource development (green boxes, Figure 4; Lautze et al. 2017b). In addition, I used the geothermal prospecting criteria of: (1) Cl/Mg ratio in excess of the of seawater value of 15 (Thomas 1987), (2) dissolved silica >65 ppm (Fournier 1982), (3) well water temperature above that of the mean annual surface temperature at the wellhead (Lautze et al. 2017a), (4) location on or near calderas, faults, and volcanic rifts, and (5) the presence of hydrothermal alteration mineralogy in proximity to a well or in well logs. I applied no weight to individual criteria, nor did I require all criteria be met.

I also determined whether each well was anomalous by comparing its values for the criteria above to known geothermal resources (which I term calibration sites), looking for similarities that could be interpreted as direct or dilute evidence for a geothermal resource. Hawai'i has only one developed geothermal resource for comparison, at PGV (Thomas 1987, Sorey and Colvard 1994, Hilton et al. 1997, Evans et al. 2015, Fercho et al. 2015); I therefore looked for similarities between waters at selected wells with those at several known volcanic geothermal systems outside of Hawai'i. These calibration sites are the Azores (Cruz and Franca 2005), Indian Ocean 'Black Smokers' (Gamo et al. 2001), the Reykjanes Peninsula, Iceland (Arnorsson 1978, Berehannu 2014), and Ladolam-Lihir, New Guinea (Simmons and Brown 2006). I selected these locations because of their association with active volcanism and the inclusion of seawater into their thermal fluids, both of which also likely influence geothermal systems in Hawai'i. Of 5,641 reported water wells in Hawai'i, only 1507 had any information on one or more of the parameters listed in the previous paragraph (University of Hawai'i 2015). I ultimately selected 66 wells based on the geochemical, geologic, and structural criteria (Table 1).

## 2.2 Explanation of Prospecting Parameters Used

Dissolved chloride in water can come from magmatic volatiles, dissolution of chloride-bearing minerals such as halite, and/or seawater mixing into the thermal system (Trusdell 1989).

Chloride is conservative once in a geothermal system, as very few chloride-bearing minerals precipitate from groundwater even at elevated temperature (Reyes 1990). Dissolved magnesium can come from low-temperature dissolution of mineral phases such as forsterite (Crundwell 2014). At elevated temperatures, and depending on reservoir characteristics such as pressure, pH, and eH,  $Mg^{2+}$  will precipitate at  $>25^{\circ}C$  into smectites and brucite (Reyes 1990, Templeton and Ellison 2020), at  $>150^{\circ}C$  in magnesite (Zhang et al. 2000), and at  $>200^{\circ}C$  into chlorite (Seyfried and Mottl 1982, Zierenberg et al. 1988). Because chloride remains dissolved in all but the highest temperature environments, but  $Mg^{2+}$  precipitates, elevated Cl/Mg ratios can be proxies for presence of geothermal resource (Thomas 1987). At PGV for example, the ratio of dissolved Cl/Mg is  $>10,000$ , far above the seawater value of 15 (Thomas 1987). None of the calibration sites with water temperatures above  $80^{\circ}C$  had a Cl/Mg below 15 (see supplemental file).

However, the relationship between increasing temperature and increasing Cl/Mg is not linear, and varies by calibration location. At temperatures below  $80^{\circ}C$ , there is no single trend for Cl/Mg values, and this may be because Cl/Mg can remain high in waters that were once hot but have now cooled, as long as they have not mixed substantially with water high in  $Mg^{2+}$ . Seawater contamination or mixing with  $Mg^{2+}$  bearing water will drop the ratio to that at or below seawater. Cl/Mg is useful, but cannot be used alone when in search of blind geothermal systems, because it is most likely that thermal waters from such a system will be first found distally from a resource, and in dilution with ambient groundwater or seawater. This approach may not be conservative in the case of mixing of water sources, as both ions can be increased or decreased in concentration depending on the chemistry of the mixing water, and only ratio values above 15 can be considered as informative.

Dissolved silica is a common component in most groundwater, and its concentration is heavily temperature dependent (Fournier 1982). Anomalously high silica can persist in ambient groundwater that has mixed with geothermal fluids, or in geothermal fluids that have cooled, due to the slow reaction kinetics of silica precipitation (Rimstidt and Barnes 1980). From statewide data, I consider 65 ppm dissolved silica to be the upper limit of background silica concentration,

and anything above 65 ppm to be anomalous. Because of the slow kinetics of silica precipitation out of water, dissolved silica concentrations will decrease slowly in a given body of water, but silica is still effected by both transport and mixing of waters, and so it is not conservative.

For wells with legacy temperature data, I compared the well water temperature to the mean annual ground surface temperature at the well head (Giambelluca et al. 2014, Lautze et al. 2017a). Waters are typically recharged at temperatures below that of the ground surface temperature at the well head because the majority of Hawaiian groundwater originates from orographic rain, driven by increasing elevation and necessarily falling temperatures. Wells without any geothermal contribution will have a temperature lower than or equal to the ground surface temperature, partially from cold recharge, and also due to groundwater thermal equilibration with the surrounding rocks. Any wells where the water temperature is higher than the mean summer ground surface temperature at the wellhead were considered anomalously warm. This method is an exclusive means for finding target wells because low enthalpy systems (low heat/mass flux), or systems experiencing a high degree of dilution are excluded from being informative.

<b>Well Name</b>	<b>Island</b>	<b>Structure</b>	<b>Silica ppm</b>	<b>Cl/Mg</b>	<b>Well Temp °C</b>
Lanai Well 3a	Lānaʻi	Rift	32	2.37	22.7
Lanai Well 4	Lānaʻi	Caldera	24.73	2.75	18.9
Lanai Well 6	Lānaʻi	Rift	23.65	2.94	19.8
Lanai Well 1	Lānaʻi	Caldera	40.32	3.76	28.1
Lanai Well 15	Lānaʻi	Caldera	37.16	3.97	25.8
Lanai Well 9	Lānaʻi	Caldera	46.36	4.01	N.D.
Lanai Well 14	Lānaʻi	Caldera	44.89	4.14	29.8
Lanai Well 8	Lānaʻi	Rift	31.74	45.48	22.9
Lanai Well 13	Lānaʻi	Rift	N.D.	N.D.	45
Lanai Well 10	Lānaʻi	Caldera	N.D.	N.D.	43
Keanu	Oʻahu	Rift	N.D.	N.D.	N.D.
Oceanic Institute	Oʻahu	Rift	N.D.	N.D.	27
Waimanalo III	Oʻahu	Rift	N.D.	N.D.	24.9
Lualualei-PVT 1	Oʻahu	Rift	90.2	9.4	28.4
Lualualei Deepwell	Oʻahu	Caldera	97.3	3.81	24
Schmidt 2006	Oʻahu	Caldera	N.D.	N.D.	27.6
Waianae III-1	Oʻahu	Caldera	N.D.	N.D.	25
Waianae III-2	Oʻahu	Caldera	N.D.	N.D.	25.3
Makaha I	Oʻahu	Rift	56	3	24.8
NSLF-03	Oʻahu	Rift	N.D.	N.D.	25.7
Honolulu International Country Club	Oʻahu	Rejuv.	46	4.5	21.7
Kaimuki Sta Deep Monitor	Oʻahu	Rift	16	23.3	N.D.
Halawa Deep Monitor	Oʻahu	Rejuv.	39.2	6.7	22.7
Waimanalo II	Oʻahu	Rift	N.D.	N.D.	24.9

<b>Well Name</b>	<b>Island</b>	<b>Structure</b>	<b>Silica ppm</b>	<b>Cl/Mg</b>	<b>Well Temp °C</b>
Waialae SH Deep Monitor	O'ahu	Rift	N.D.	N.D.	N.D.
Well 4	O'ahu	Caldera	N.D.	N.D.	N.D.
Sherrill	O'ahu	Caldera	N.D.	N.D.	21.1
Ukumehame	Maui	None	71	19.77	33
Sugar Way	Maui	None	N.D.	N.D.	32.2
Ukumehame 3	Maui	None	N.D.	N.D.	25.9
Wakiu-Hana Ranch	Maui	Rift	20.5	25.6	21.5
Wananalua	Maui	Rift	0	8.29	21
Kaeleku-Hana	Maui	None	20.9	2.38	20.1
Haiku-Baldwin	Maui	Rift	N.D.	N.D.	21.7
Hamilton	Maui	Rift	N.D.	N.D.	26.1
Kalepa-Starr	Maui	None	N.D.	N.D.	20
Waikii 1	Hawai'i	None	68.4	1	31.7
Parker 5	Hawai'i	None	71	2.73	26.7
Hawaiian Ocean View Estates	Hawai'i	Rift	44.7	5.42	27.44
Parker 4	Hawai'i	None	67	1.62	26.7
Parker 1	Hawai'i	None	67	0.62	27.8
Kawaihae Deepwell 1	Hawai'i	None	66	11.25	27.2
Kawaihae Deepwell 2	Hawai'i	None	77	9.73	26.4
Mauna Kea Beach Hotel 4	Hawai'i	None	N.D.	N.D.	N.D.
Kawaihae 2	Hawai'i	None	30	18.13	26.1
Kawaihae 3	Hawai'i	None	84	7.9	35.6
Kawaihae	Hawai'i	Rift	N.D.	N.D.	N.D.
Puanui 1	Hawai'i	None	N.D.	N.D.	30.28

Well Name	Island	Structure	Silica ppm	Cl/Mg	Well Temp °C
Kalaoa Deepwell	Hawai'i	Rift	N.D.	N.D.	23.3
South Point Tank	Hawai'i	Rift	N.D.	N.D.	22.61
Ninole-Wailau 1	Hawai'i	Rift	N.D.	N.D.	N.D.
Kalaoa Keopu Deep Monitor	Hawai'i	None	N.D.	N.D.	N.D.
Kau Deepwell	Hawai'i	Rift	N.D.	N.D.	25.8
Pohakuloa TH	Hawai'i	None	N.D.	N.D.	N.D.
Kaupulehu Irrigation 6	Hawai'i	None	N.D.	N.D.	23.6
Waiaka Gulch TH	Hawai'i	Rift	N.D.	N.D.	N.D.
Koloa D	Kaua'i	Rift	65.97	3.32	23.9
Kalaheo Deep Well 1	Kaua'i	Rejuv.	46.89	2	N.D.
Puhi 3	Kaua'i	Caldera	24.76	2.45	23.6
Puhi 4	Kaua'i	Caldera	36.22	2.23	23.2
Kalepa Ridge	Kaua'i	Caldera	81.47	2.32	25.4
Lawai 2	Kaua'i	Rejuv.	54	1.95	N.D.
Kapaa Homesteads	Kaua'i	Rift	31	1.97	22.8
Honuhonu	Kaua'i	Rejuv.	N.D.	N.D.	27.8
Hanamaulu 4	Kaua'i	Caldera	45.82	1.21	24.9
Kawaihae-DHHL	Hawai'i	Rift	N.D.	N.D.	29

Table 1. Well names, island location, associated structural feature if present (Rejuv. is abbreviated for rejuvenation stage volcanic center), SiO<sub>2</sub> concentration, Cl/Mg ratio, and temperature. N.D. where no data were available. Well names are listed as they are spelled in the Commission on Water Resource Management database (University of Hawai'i 2015).

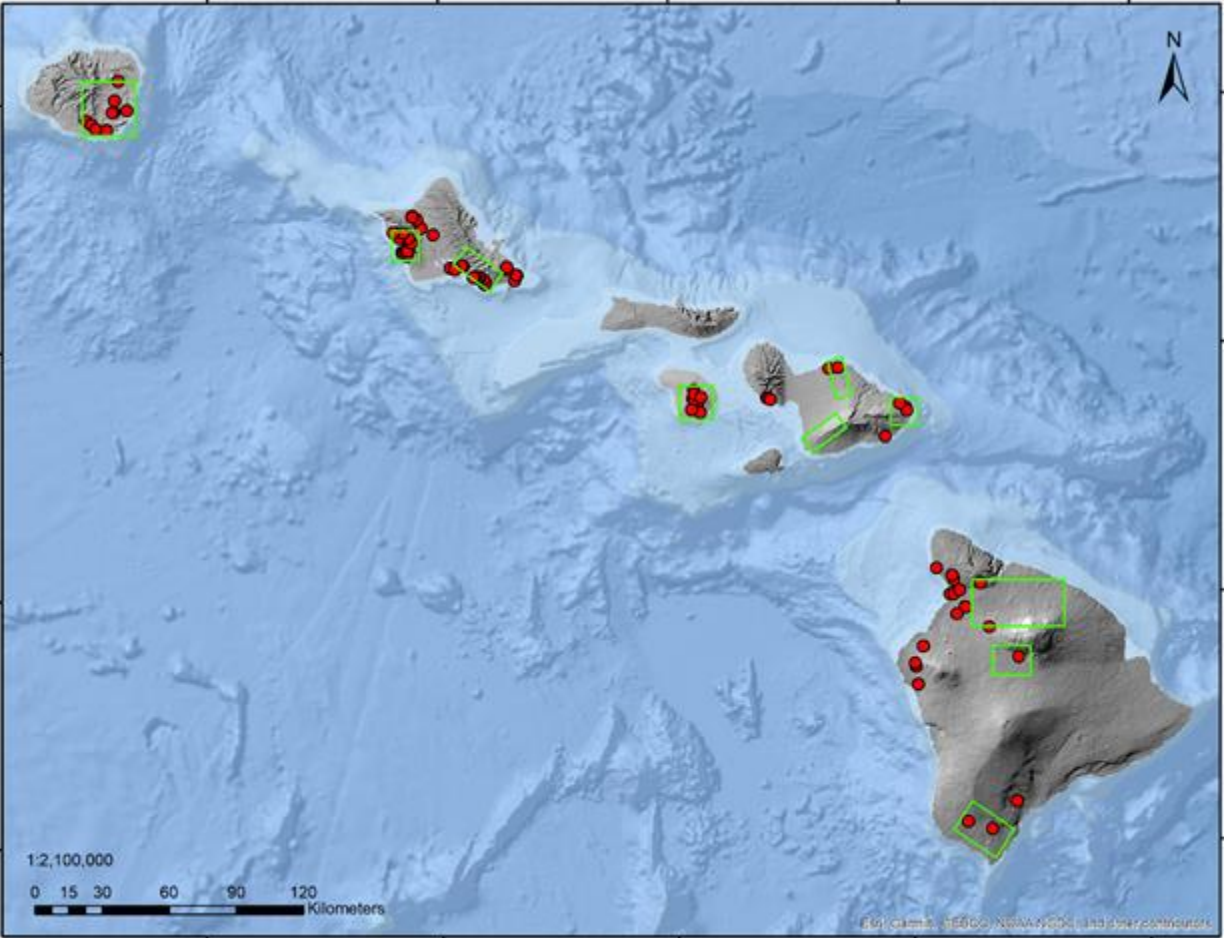


Figure 5. Map of Play Fairway areas of interest as (green boxes; Lautze et al. 2017b). The 66 target wells of this study are shown as red points.

I plotted geothermal indicators from the target wells and calibration sites listed above in order to make comparisons between the known trends at the calibration sites and my targeted wells.

These geothermal indicators are: Cl/Mg vs temperature, dissolved SiO<sub>2</sub> vs Cl/Mg, dissolved K<sup>+</sup> vs Cl/Mg, dissolved Mg<sup>2+</sup> vs dissolved K<sup>+</sup>, and dissolved SO<sub>4</sub><sup>2-</sup> vs Cl/Mg. These comparisons were selected due to the availability of data on those parameters. Some of the calibration geothermal systems showed the expected relationships, such as a positive correlation dissolved SiO<sub>2</sub> and temperature, or negative correlation between Mg<sup>2+</sup> and both Cl<sup>-</sup> and K<sup>+</sup>. However, these relationships were broad, and only consistent for well waters above 35°C when applied to Hawaiian well waters other than those at PGV (e.g. Figure 6). Because of these unclear patterns, and little overlap with Hawaiian waters, I show only Figure 6 here, excluding the other plots.

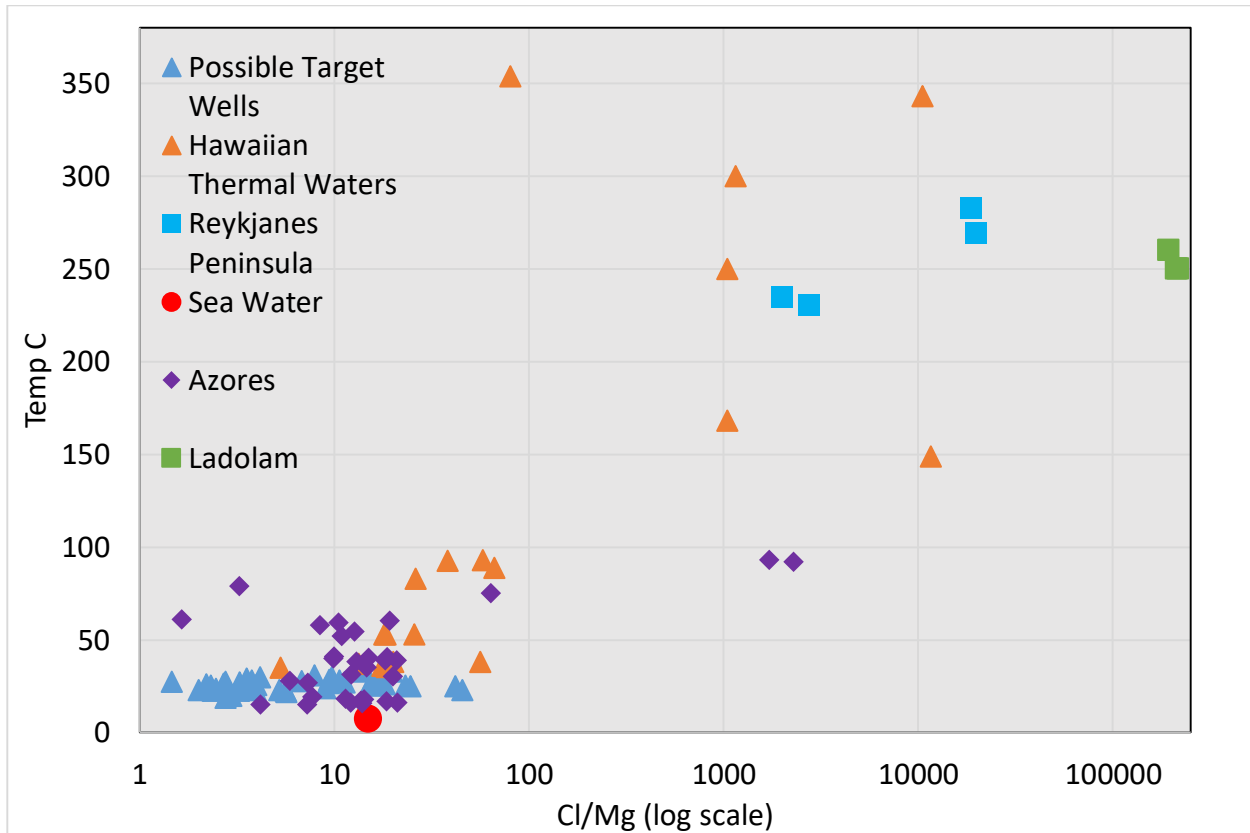


Figure 6. A set of potential well targets, before selection of the final 66, compared to calibration cases. The range of Cl/Mg varies by 5 orders of magnitude for known high temperature sites. With a few exceptions from the Azores, all wells with water temperatures above 50°C have Cl/Mg above that of seawater. However, the highest Cl/Mg ratio does not correlate with the highest temperature. The warmest potential well targets (blue triangles) shown here do have Cl/Mg at or above that of sea water, but the highest Cl/Mg target wells show ambient groundwater temperatures.

### 2.3 Sample Collection and Analysis

I was granted access to sample 23 wells. Several of these wells were sampled as replacements for unavailable nearby wells, or as opportunities not in the original 66 targets. Collection occurred from October 2018 to February 2020. The 23 samples were analyzed for  $^2\text{H}$ , He, Ne, Ar, Kr, Xe,  $\delta^{18}\text{O}\text{-H}_2\text{O}$ ,  $\delta\text{D}\text{-H}_2\text{O}$ , As, B, Ba, Be, Br, Ca, Cd, Cl, Co, Cr, Cu, Fe, F, K, Li, Mg, Mn, Mo, N, Na, Ni, P, Pb, Re, Sb, Se,  $\text{SiO}_2$ ,  $\text{SO}_4$ , Sr, U, V, and Zn (see supplemental file). In addition, temperature, pH, and conductivity were measured in the field at the time of sampling.

I collected noble gas samples using copper refrigeration tubes that are 40 cm long with a diameter of 2 cm. This is standard equipment for such sampling (Weiss 1968, Aeschbach and Solomon 2012,). The tubes were attached to pumping wells with a standard hose bib, or a copper standpipe using brass or polymer fittings and hose clamps, and mounted to an aluminum chassis to prevent bending of the tube. A hose valve attached to the discharge end of the tubes ensured that I was able to create an increasing pressure gradient toward the well to prevent air from entering the tube end. Water was allowed to flow through the copper tube for five minutes to ensure that any bubbles entrapped in the sample line were purged. Once purged, I sealed the tubes using custom-milled mild steel clamps and bolts, tightened onto the tubes with a battery drill and ratchet. Care was taken at each well sampled to ensure that all seals were airtight, no bubbles were able to enter the water, and no water could leak from the sample line. In one case, I deployed a specialized sampler down a pump-less well. This sampler used the same type of copper tubes, but was fitted with brass check valves on brass compression fittings at the ends, as conceptualized by Donald Thomas at the University of Hawai'i. The check valves open only once a pre-determined pressure (in this case equivalent to a depth of 22 feet below the water surface) is exerted on them, and seal once pressure equilibrium has been reached. This allows sampling of water at that specified depth (Figure 7).



Figure 7. Several filled and sealed copper tube samplers. The experimental check-valve sampler is shown, second from top, with check valves removed, but compression fittings still on.

Noble gas samples from the island of Lāna`i were analyzed by the GEOTOP lab at the University of Quebec, Montreal (Mejean et al. 2020). Samples, from Hawai`i, O`ahu, and Kaua`i were analyzed by the USGS Noble Gas Lab (Hunt 2015), with additional samples from Kaua`i analyzed by the Noble Gas Lab at the University of Utah (Stanley et al. 2009, Matsumoto et al. 2017). In all cases noble gases were extracted through a multi-step vacuum system and purified through multiple cryogenic traps. Purified and separated gases were then sent to a dedicated mass spectrometer. The common standard of atmosphere is used by each lab.

I collected  $^2\text{H}$  and  $^{18}\text{O}$  samples through a Tygon tube attached to a sampling syringe, inserted into a discharging hose bib at the wellhead. I then passed the water from the filled syringe

through a 0.22-micron filter and into acid-washed 60 mL EPA borosilicate glass vials with no headspace. These samples were analyzed by the University of Hawai`i, Mānoa Biogeochemical Stable Isotope Facility, where analysis is completed on a L2130-I Picarro cavity ring-down spectrometer. Samples are normalized to VSMOW using desalinated Kona deep-water, lab deionized water, and Mauna Kea Snow, which are calibrated inter-lab to SLAP-2, VSMOW-2, and GISP supplied from the International Atomic Energy Agency (Godoy et al. 2012). Additional water isotope samples from Hawai`i island and O`ahu were analyzed at the University of Utah Stable Isotope Facility (SIRFER), with the same type of Picarro spectrometer as above, using laboratory internal standards.

Dissolved trace metals and ions were sampled in the same way as  $^2\text{H}$  and  $^{18}\text{O}$ , and analyzed by the Water Resource Research Center Analytical Chemistry Laboratory at the University of Hawai`i, Mānoa. Trace metal analyses followed EPA method 200.7, using a Thermo Scientific iCAP 6300 Duo ICP (Martin et al. 1994). Major ions were determined using dual Dionex ICS-1100 Ion Chromatographs operated at ambient temperature at a flow rate of 1.0 mL/min, and detection by suppressed conductivity. Anions were separated on a Dionex IonPac AS14A column with 8 mM  $\text{Na}_2\text{CO}_3$ /1 mM  $\text{NaHCO}_3$  eluent. Cations were separated on a Dionex IonPac CS12A column with 20 mM  $\text{CH}_3\text{SO}_3\text{H}$  eluent.

## 2.4 Equations

A number of standard equations are used in noble gas interpretations. These standardizations simplify comparisons between noble gas reservoirs and the processes that can fractionate noble gas isotopes by normalization to the atmosphere and by considering isotopic ratios instead of volumes of each isotope. These largely serve as visualization aides. I present helium data as the following:

$$R/R_a = \frac{\left(\frac{^3\text{He}}{^4\text{He}}\right)_{\text{sample}}}{\left(\frac{^3\text{He}}{^4\text{He}}\right)_{\text{atmosphere}}}$$

Where  $R_a = 1.39 \times 10^{-6}$ ,  $R/R_a$  of the atmosphere is 1, and ASW  $R/R_a$  at 20°C is 0.98.  $R/R_a$  is useful in making comparisons of relative helium isotope enrichment between potential helium source reservoirs, by normalizing all measurements to the atmosphere (Craig et al. 1978).

A correction for excess air (EA) from bubble entrapment at the time of ground infiltration by meteoric water can be made. This is an important correction because all ground waters will have some component of excess air that will interfere with true groundwater equilibrium values, as well as any subsequently added noble gases. This is defined as  $R_c$  (Craig 1978, Sano 2006).

$$R_c/R_a = \left( \frac{R}{R_a} \times \frac{{}^4\text{He}}{{}^{20}\text{Ne}}_{\text{normalized}} - 1 \right) / \left( \frac{{}^4\text{He}}{{}^{20}\text{Ne}}_{\text{normalized}} - 1 \right)$$

Where  $[{}^4\text{He}]/[{}^{20}\text{Ne}]_{\text{normalized}} =$

$$\frac{\left( \frac{{}^4\text{He}}{{}^{20}\text{Ne}} \right)_{\text{sample}}}{\left( \frac{{}^4\text{He}}{{}^{20}\text{Ne}} \right)_{\text{atmosphere}}}$$

and  $[{}^4\text{He}]/[{}^{20}\text{Ne}]_{\text{atmosphere}}$  is 0.288 for the atmosphere and 0.244 for ASW at 20°C. Both ASW and atmosphere  $[{}^4\text{He}]/[{}^{20}\text{Ne}]$  are used to calculate  $R_c/R_a$  using the measured range of uncertainty from each sample as reported from laboratory analysis. The  $R_c/R_a$  reported here is the average of values from both ASW and atmosphere, over the full  $1\sigma$  error. The resulting uncertainty is found, by calculation of the standard deviation of all errors for both an ASW and atmospheric value of  $[{}^4\text{He}]/[{}^{20}\text{Ne}]$  (Sano 2006):

$$\sigma_{\text{total}} = \sqrt{\sigma_{\text{corrected}}^2 + \sigma_{\text{measured}}^2}$$

The excess air correction is not applicable for measured sample values approaching  $[{}^4\text{He}]/[{}^{20}\text{Ne}]_{\text{normalized}}$  of 1, as it can cause negative correction values, or division with values of  $<1$  in the denominator of the  $R_c$  equation, both of which will yield unrealistic results. This correction operates under an assumption that all Ne in a sample is effectively from the atmosphere.

While  $R/R_a$  and  $R_c/R_a$  give a clear representation of relative  $^3\text{He}$  enrichment in a sample relative to the atmosphere, a separate method of looking at relative  $^4\text{He}$  enrichment is required. The F-enrichment factor is used to describe any individual noble gas isotope relative to the atmosphere (Kennedy et al. 1988). Regardless of the isotope being investigated,  $^{36}\text{Ar}$  is the common denominator.  $^{36}\text{Ar}$  is dominantly primordial and shows limited fractionation between atmosphere and other reservoirs.  $^{36}\text{Ar}$  is also relatively abundant at  $3.14 \times 10^{-5}$  in the atmosphere, which is an order of magnitude more abundant than He in the atmosphere (Ozima and Podosek 2002).

$$F(^4\text{He}) = \frac{\left(\frac{^4\text{He}}{^{36}\text{Ar}}\right)_{\text{sample}}}{\left(\frac{^4\text{He}}{^{36}\text{Ar}}\right)_{\text{atmosphere}}}$$

Where  $[\text{He}]/[\text{Ar}]_{\text{atmosphere}} = 0.167$ ,  $F(^4\text{He})$  of the atmosphere is 1, and ASW at  $20^\circ\text{C}$  is 0.25. The F-enrichment factor is useful for determining the relative increase in  $^4\text{He}$  in a sample, independently from  $^3\text{He}$ .

Mixing curves between ASW at  $20^\circ\text{C}$  and between various noble gas reservoirs (crust, mantle, plume, atmosphere, ocean) are simple two component mixture calculations achieved by incrementally adding end-member components. This is expressed as:

$$\text{New } R/R_a = \frac{((A \times R \times X) + B)}{(C + A)} \Bigg/ R_a$$

Where A is the total volume of helium added, R is the ASW ratio of  $^3\text{He}/^4\text{He}$  ( $1.356 \times 10^{-6}$ ), X is any non ASW reservoir (e.g. 0.01 for crust, 8 for upper mantle, 35 for plume), B is the  $^3\text{He}$  volume of ASW at  $20^\circ\text{C}$  ( $6.094 \times 10^{-14}$  cc/g), C is the  $^4\text{He}$  volume of ASW at  $20^\circ\text{C}$  ( $4.48 \times 10^{-8}$  cc/g) and  $R_a$  is atmospheric  $^3\text{He}/^4\text{He}$  ( $1.384 \times 10^{-6}$ ). This equation provides the new  $R/R_a$  after mixing a given volume of helium at a specific  $R/R_a$ . This process is then repeated until the full range between the end members is reached, allowing for a mixing curve to be plotted. In addition,  $F(^4\text{He})$  must also be calculated by adding the same incremental volume at each step as was added to get each new  $R/R_a$ :

$$New F(^4He) = \frac{A + C}{D} / E$$

Where A and C are the same as above, D is the  $^{36}Ar$  value for ASW at 20°C, and E is the atmospheric ratio for  $^4He/^{36}Ar$  (0.166).

Modeling a potential  $R/R_a$  for the oceanic lithosphere beneath the Hawaiian Islands required making some assumptions about the age, uranium and thorium concentration, initial  $R/R_a$ , and initial helium volumes. The uranium and thorium concentrations I used are 0.15 ppm and 0.06 ppm respectively, and are the average of 8 values of U and Th collected by several researchers (Staudigel et al. 1996, Hart et al. 1999, Bach et al. 2001, Bach et al. 2003, , Kelly et al. 2003). The initial  $R/R_a$  for calculating the current  $R/R_a$  is the upper mantle mean of 8 (Graham 2002), and the volumes for  $^3He$  and  $^4He$  are  $7*10^{-13}$  cc/g and  $6.25*10^{-08}$  cc/g respectively (Sano and Fischer 2013). These values were put into the equation below (Ballentine and Burnard 2002):

$$^4He \text{ atoms per gram of lithosphere} = T*((3.115*10^6+1.272*10^5)*[U])+((7.710*10^5)*[Th])$$

The results from this equation are converted from atoms to cc/g per gram, added to the initial  $^4He$  volume, and combined with a constant  $^3He$  volume to find a new  $R/R_a$  for an oceanic lithosphere that is ~92 million years old (Müller et al. 2008). The resulting  $R/R_a$  and calculated initial  $F(^4He)$  of 694 were then used to form a radiogenic lithosphere reservoir mixing line.

Finally, the potential tritiogenic  $^3He$  influence was modeled. Because tritium is produced in the atmosphere and readily oxidizes into  $H_2O$ , it can be entrained into groundwater, yielding significant non-geothermal  $^3He$ . If 1 tritium unit (1 TU = 1  $^3H$  atom per  $10^{18}$  H atoms) of tritium per gram of  $H_2O$  fully decays, it will yield  $4.012*10^{-14}$  cc/g  $^3He$  (Porcelli et al. 2002). At low total helium volumes this could be a significant contribution to  $R/R_a$  values, obscuring interpretations.

### 3. Results

#### 3.1 Statewide Overview

Due to access and time limitations noted above, I sampled 23 of my 66 well targets. I supplemented the data from this project with results from an exploration by the geothermal power company Ormat Technologies Inc., which runs PGV (Fercho et al. 2015), and with data published by the USGS Hawaiian Volcano Observatory on gas from the Sulphur Banks at Kīlauea (Hurwitz et al. 2020). During the course of sampling and lab analysis, several samples were contaminated, and made unusable. These samples are excluded from this study, and are not reported here.

Statewide,  $R/R_a$  values ranged from 0.37 to 15.56,  $R_c/R_a$  from 0.20 to 15.78, and  $F(^4\text{He})$  from that of ASW to 120.39 (Table 4). Each island shows a variability in noble gas characteristics, but other than at Kīlauea, the maximum  $R/R_a$  falls within the same values of the upper mantle (6.5-9.5). Similarly,  $F(^4\text{He})$  drops towards that of ASW on progressively older islands.  $^{40}\text{Ar}/^{36}\text{Ar}$  did not vary appreciably ( $\pm 5$ ) from ASW at 295, with the exception of one sample from Lāna‘i at 320.  $^{20}\text{Ne}/^{22}\text{Ne}$  did not vary from ASW (9.8) except for at the Sulphur banks, where a value of 10.17 was reported by the USGS.  $F(^{22}\text{Ne})$ ,  $(^{84}\text{Kr})$ , and  $F(^{132}\text{Xe})$  were all near ASW concentrations, except at the Sulphur Banks fumaroles, which were enriched in He and Ne, and depleted in Kr and Xe. Errors for noble gas samples are analytic in nature and are reported by the analysis lab. No clear trends emerged in the trace metals and ions, and they will not be discussed in detail, but are listed in the supplemental file. Water isotope data for  $\delta^2\text{H}_{\text{VSMOW}}$  and  $\delta^{18}\text{O}_{\text{VSMOW}}$  ranged from -68.23 to -12.40‰ for  $^2\text{H}$ , and -9.66 to -4.4‰ for  $^{18}\text{O}$  (Table 2, Figure 9).

Sample Name	$\delta^{18}\text{O}$ (‰)	$\delta\text{D}$ (‰)	pH	Temp °C
Lanai Well 1	-4.40	-23.20	7.53	28.89
Lanai Well 10	N.D.	N.D.	N.D.	40
Lanai Well 14	-4.10	-22.00	7.23	30.3
Lanai Well 15	-4.10	-22.30	7.24	26
Lanai Well 2	-3.70	-18.50	8	19.8
Lanai Well 6	-4.40	-20.20	8.3	19.6
Lanai Well 9	-4.20	-22.50	N.D.	35
Hanamaulu 4	-3.00	-12.40	8.49	24.9
Maalo Rd Mon	N.D.	N.D.	N.D.	N.D.
Pukaki Res Mon	N.D.	N.D.	N.D.	N.D.
NE Kilohana Mon	-3.20	-12.50	N.D.	N.D.
Kilohana A	-3.23	-12.47	8.54	25.3
Kapaa Homestead	N.D.	N.D.	8.04	24.6
Puhi 4	N.D.	N.D.	6.51	22.7
Hanamaulu	-3.05	-12.36	7.34	24.5
Lawai 2	N.D.	N.D.	6.99	22.2
Kalaheo 1	N.D.	N.D.	6.83	21.5
Koloa C	N.D.	N.D.	6.59	22.9
Waikii Ranch	-9.66	-68.23	8.34	27.7
Lalamio C	-5.40	-29.64	8.42	26.1
Parker 4	-5.60	-31.90	8.38	27.2
Hawaiian Ocean View	-7.57	-50.38	8.73	28
Naalehu DW	-4.13	-20.36	7.96	19.4
Pahala DW 1	-4.81	-25.64	8.27	17.7
Pahoa DW 2	-3.57	-14.76	8	23
Kalapana DW 1	-3.35	-13.74	8.2	23
Puu Lani	-7.67	-50.97	8.69	23.4
DW-3	-6.83	-42.29	8.36	28.8
LLL DW	-4.50	-24.69	8.18	24.85
Sherill Well	-4.04	-20.31	8.87	N.D.
Royal Hawaiian GC 4	-4.04	-20.31	N.D.	25.1

Table 2. Stable Isotope data for water collected during this study. pH and temperature are also provided, and were measured in the field. This information is shown graphically in Figure 9.

### 3.2 Model Results

I calculated the potential contributions of  $^3\text{He}$  from tritium to determine whether this process significantly affected my  $^3\text{He}$  results (Table 2). Historic TU on Hawai‘i, where continuous data are most complete (Lau and Hailu 1968, Lau and Hufen 1973, Kennedy 1985, Scholl et al. 1995), ranges from a maximum of 373 TU in 1964 as a result of atmospheric atomic weapons testing, gradually down to a TU of 2-3 in the 2000s, which is the assumed background production value. With a half-life of 12.43 years (Kaufman and Libby 1954), about 12 TU from the 1964 bomb peak would be stored in closed system waters today, and the tritiogenic  $^3\text{He}$  ingrown during the time since the bomb peak would yield an  $R/R_a$  of 15.96 from an ASW starting value of  $R/R_a$  0.98. However, given that Hawaiian aquifers are open systems, no  $R/R_a$  that high could be entirely tritiogenic due to mixing with younger recharge waters. The open system tritiogenic  $^3\text{He}$  values in modern Hawaiian waters will thus be a constant mix, diluting from higher past TU towards the time integrated contribution from modern 2-3 TU waters, and lower tritiogenic  $^3\text{He}$  composition. The maximum measured TU during the last 35 years, which is the average groundwater age of Hawai‘i, is 5.4 TU (Scholl et al. 1995). The closed system total decay of 5.4 TU results in an  $R/R_a$  of 1.2. The 35-year average TU is 2.5, with a resultant total decay to  $R/R_a$  of 1.1. Given that groundwater age is not the same in all Hawaiian aquifers, I estimate the highest expected  $R/R_a$  likely to be found in Hawai‘i to be below 3, as the 35 year closed system maximum is far lower, but there is potential for mixing of older waters. On a mixing model of  $R/R_a$  plotted against  $F(^4\text{He})$ , purely tritiogenic  $^3\text{He}$  input will move the  $R/R_a$  vertically away from ASW, with no effect on  $F(^4\text{He})$ . However, tritium components cannot be separated from  $R/R_a$  values that co-vary with  $F(^4\text{He})$ , as is the case for crust, mantle, and plume reservoirs.

TU	Tritiogenic $^3\text{He}$	R/R <sub>a</sub>	F( $^4\text{He}$ )
0	6.094E-14	0.98	0.256
1	6.343E-14	1.02	0.256
2	6.592E-14	1.06	0.256
3	6.840E-14	1.10	0.256
4	7.089E-14	1.14	0.256
5.4	7.438E-14	1.20	0.256
10	8.582E-14	1.39	0.256
100	3.098E-13	5.00	0.256
300	8.074E-13	13.03	0.256
373	9.890E-13	15.96	0.256

Table 3. A range of real TU values for Hawaiian waters, and the R/R<sub>a</sub> that results for total decay of TU in a closed system. The highest recorded TU is from 1964, and represents a substantial contribution from the “bomb peak”. TU 5.4 is the maximum value within the last 35 years, and the 35 year average is 2.5.

Radiogenic  $^4\text{He}$  from the decay of uranium and thorium is introduced to water samples through diffusion from and dissolution of minerals at elevated temperature, and any such  $^4\text{He}$  will therefore influence helium values, given enough volume. The young basalts of the Hawaiian Islands possess neither the age, nor U and Th concentrations, to influence the helium values presented here. In order to prove this, I calculated the radiogenic  $^4\text{He}$  input for an average Hawaiian basalt, with 0.3 ppm U and 0.8 ppm Th (Larsen and Gotfried 1960). The model allows U and Th to decay into a closed system with the values of  $^3\text{He}$  and  $^4\text{He}$  from Lō‘ihi seamount (Kurz 1983). In this case,  $^3\text{He}$  is fixed, while  $^4\text{He}$  increases with time. R/R<sub>a</sub> dropped from an initial value of 27 to 18.9 after 5 Ma, which is the approximate age of the island of Kaua‘i (McDougall 1979), the oldest island in my study. This represents a significant increase in  $^4\text{He}$  volume in the modeled rock, and an increase in F( $^4\text{He}$ ). Given these results, samples influenced by radiogenic components from the rocks comprising the islands themselves would always have considerably higher R/R<sub>a</sub> than the lowest R/R<sub>a</sub> values seen in my study. Because some of my results fall below an R/R<sub>a</sub> of 1 and below mantle-ASW mixing lines, a radiogenic input of  $^4\text{He}$  is required with an R/R<sub>a</sub> lower than that of any aged Hawaiian Island. I considered another source of  $^4\text{He}$ , the oceanic crust. Using the same equations from my methods, I modeled a closed system

ingrowth of radiogenic  $^4\text{He}$  in the oceanic crust. After 90 Ma,  $R/R_a$  in these modeled rocks dropped to 0.27, which is in range of my lowest  $R/R_a$  samples (Table 3).

Time	$^4\text{He}$ cc/g Ingrown	$^3\text{He}$ cc/g	$R/R_a$
100000	1.98E-09	7E-13	7.75
200000	3.96E-09	7E-13	7.52
300000	5.95E-09	7E-13	7.30
1000000	1.98E-08	7E-13	6.07
2000000	3.96E-08	7E-13	4.90
3000000	5.95E-08	7E-13	4.10
10000000	1.98E-07	7E-13	1.92
20000000	3.96E-07	7E-13	1.09
30000000	5.95E-07	7E-13	0.76
90000000	1.78E-06	7E-13	0.27
100000000	1.98E-06	7E-13	0.24
1000000000	1.98E-05	7E-13	0.03

Table 4. Ingrowth of radiogenic  $^4\text{He}$  into an average composition oceanic lithosphere over time, and the evolving  $R/R_a$  from this ingrowth in a closed system. Blue highlight represents the approximate age of the Oceanic Lithosphere underlying the Hawaiian Islands, and its modeled  $R/R_a$ .

Well Name	Island	R/Ra	±	Rc/Ra	±	F(4He)	±
Pahoa DW#2	Hawai'i	1.60	1.06E-02	1.85	8.04E+00	0.29	3.11E-04
HOVE B	Hawai'i	2.58	1.71E-02	16.11	8.90E+00	0.37	4.87E-04
DW-3	Hawai'i	1.00	6.65E-03	1.01	1.70E-02	0.29	3.00E-04
Waikii Well 1	Hawai'i	1.40	9.28E-03	1.16	5.29E+00	0.31	3.37E-04
Puu Lani	Hawai'i	1.82	1.21E-02	1.82	1.09E+01	0.29	3.05E-04
Pahala DW 1B	Hawai'i	1.05	7.00E-03	-0.26	1.77E+00	0.26	2.45E-04
Naalehu DW	Hawai'i	1.07	7.12E-03	-340.2	1.45E+03	0.26	2.42E-04
Lalamio C	Hawai'i	1.12	7.47E-03	7.37	2.39E+01	0.28	2.83E-04
Kalapana DW-1	Hawai'i	1.11	7.37E-03	21.06	8.11E+01	0.27	2.69E-04
SB18-04B	Hawai'i	13.41	1.34E-01	13.65	1.36E-01	120.39	1.80E+00
SB18-05B	Hawai'i	15.27	1.07E-01	15.39	1.08E-01	78.70	1.58E+00
SB19-01a	Hawai'i	15.42	1.08E-01	15.62	1.11E-01	33.18	6.68E-01
SB19-01b	Hawai'i	15.56	1.09E-01	15.78	1.13E-01	32.45	6.53E-01
KS-6 Well - Gas	Hawai'i	13.73	2.85E-01	14.34	3.02E-01	8.45	4.13E-01
KS-5 Well - Gas	Hawai'i	13.82	3.02E-01	14.52	3.21E-01	6.93	2.78E-01
KS-14 Well - Gas	Hawai'i	13.76	2.65E-01	14.46	2.83E-01	7.81	3.53E-01
KS-10 Well - Gas	Hawai'i	14.42	2.73E-01	15.13	2.91E-01	8.87	4.57E-01
KS-9 Well - Gas	Hawai'i	13.97	3.05E-01	14.61	3.23E-01	8.14	3.83E-01
MW-2 Well	Hawai'i	2.42	1.17E-01	10.77	8.27E-01	0.59	1.30E-03
MW-1 Well	Hawai'i	1.69	1.49E-01	5.28	9.38E-01	0.61	1.22E-03
MW-3 Well	Hawai'i	2.80	1.97E-01	10.81	1.08E+00	0.61	1.39E-03
Well HR-4	Hawai'i	7.65	1.63E-01	8.53	1.90E-01	3.09	5.50E-02
Well HR-1	Hawai'i	8.51	1.85E-01	9.20	2.06E-01	4.10	9.79E-02
Well HR-3	Hawai'i	6.54	1.65E-01	8.02	2.15E-01	1.74	1.82E-02
Well HR-5	Hawai'i	8.19	2.30E-01	9.27	2.68E-01	2.81	4.63E-02
Kalaoa Well	Hawai'i	1.94	1.79E-01	4.53	6.96E-01	0.47	1.75E-03
Hualalai Well	Hawai'i	2.16	1.69E-01	4.47	5.18E-01	0.51	1.57E-03
Well HR-4	Hawai'i	7.64	2.04E-01	8.44	2.30E-01	3.36	3.59E-02
Well HR-1	Hawai'i	8.67	1.68E-01	9.35	1.84E-01	4.41	6.17E-02
Well HR-5	Hawai'i	8.15	2.11E-01	9.12	2.42E-01	3.06	3.01E-02
Kilohana A	Kaua'i	7.47	4.97E-02	8.81	1.40E-01	1.89	1.30E-02
Maalo Rd EXP	Kaua'i	1.31	8.73E-03	3.45	5.68E+00	0.32	3.72E-04
Lawai	Kaua'i	1.00	1.00E-02	0.90	2.67E-01	0.28	5.75E-04
Puhi 4	Kaua'i	1.01	1.00E-02	0.84	8.36E-01	0.29	6.09E-04
Hanamaulu	Kaua'i	6.92	6.90E-02	9.49	3.28E-01	1.17	9.95E-03
Kapaa	Kaua'i	1.06	1.10E-02	2.84	7.46E+00	0.33	7.92E-04
Lanai 14	Lāna'i	0.37	7.06E-01	0.20	2.00E-02	0.33	8.92E-03
Lanai 2	Lāna'i	0.84	8.07E-02	0.76	1.06E-02	1.42	3.77E-02
Lanai 1	Lāna'i	1.35	3.02E-01	1.53	2.46E-02	0.48	1.28E-02
Lanai 15a	Lāna'i	6.81	5.04E-01	10.30	4.92E-01	1.43	3.82E-02
Wailea Well #1	Maui	7.03	1.54E-01	7.63	1.70E-01	4.02	3.34E-02
Wailea Well #2	Maui	5.70	1.56E-01	7.43	2.14E-01	1.30	3.60E-03

Horse Well	Maui	2.93	9.34E-02	3.15	1.12E-01	3.56	7.32E-02
Sherill Well	O'ahu	1.04	6.89E-03	0.48	3.66E+00	0.39	5.57E-04
LLL DW	O'ahu	1.21	8.06E-03	3.59	5.20E+00	0.28	2.90E-04
RHGC 4	O'ahu	2.77	2.80E-02	22.14	1.36E+01	0.36	3.35E-04

Table 5. Helium values discussed in this paper. Well names are as they appear in the state database. Erroneous values for  $R_c/R_a$  are shown for completeness, and are the result of the limitations inherent in the  $R_c$  equation as discussed in methods. They are not used in interpretations. Errors shown are analytic in nature. Well ID numbers are provided in the supplemental file.

### 3.3 Kaua'i

I collected seven samples from Kaua'i wells. Five of these samples come from within the Līhu'e basin. The Hanamaulu well has an  $R/R_a$  of 6.92,  $R_c/R_a$  of 9.49, and  $F(^4\text{He})$  of 1.71. The Kilohana A well has an  $R/R_a$  of 7.47,  $R_c/R_a$  of 8.81, and  $F(^4\text{He})$  of 1.89. The check-valve method sample from the Ma'alo Road well had an  $R/R_a$  of 1.31, and  $F(^4\text{He})$  of 0.32. The  $R_c/R_a$  correction could not be applied to the Ma'alo Road sample and it is not clear if a check-valve sampler can be purged of air bubbles when deployed in a well, as the sample taken with it in this study was too close to atmospheric values to make the excess air correction. Further experimentation with this sampler should try to clarify that in laboratory settings. It is important to note that there was an inflow of shallow groundwater into the Ma'alo Road well, and that the check valve opened at 6.8 meters of water depth, both factors that might have diluted a stronger signal at greater well depth. The Kapa'a well has an  $R/R_a$  of 1.06, and an  $F(^4\text{He})$  of 0.33, and could not be  $R_c/R_a$  corrected. The Puhī 4 well has an  $R/R_a$  of 1.01, and  $R_c/R_a$  of 0.84, and an  $F(^4\text{He})$  of 0.29. Outside of the Līhu'e Basin, I sampled the Koloa C and Lawai 2 wells. The Koloa C well, located along a rejuvenation rift, has an  $R/R_a$  of 1.91, and an  $F(^4\text{He})$  of 0.32, and was unsuitable for the  $R_c/R_a$  correction. Lawai 2 well, not associated with a volcanic structure, has an  $R/R_a$  of 1.00, an  $R_c/R_a$  of 0.90, and an  $F(^4\text{He})$  of 0.28.

### 3.4 O'ahu

I collected three samples on O'ahu. One from the Wai'anae Caldera, and two from the Ko'olau Caldera. The Lualualei Deep well sample (LLL DW) from Wai'anae Caldera showed a very slight enrichment in  $F(^4\text{He})$  of 0.28, and an  $R/R_a$  near ASW at 1.21. Similarly, the Sherill Well

sample in the Ko‘olau Caldera had values near ASW with  $F(^4\text{He})$  of 0.39 and an  $R/R_a$  of 1.04. The Royal Hawaiian Golf Course 4 well (RHGC 4) sample had an  $R/R_a$  of 2.77, but a near ASW  $F(^4\text{He})$  of 0.36. None of the samples from O‘ahu are suitable for the  $R_c/R_a$  correction.

### **3.5 Lāna‘i**

The four samples from Lāna‘i come from within, or near the Pālāwai caldera basin. Lāna‘i well 15a has an  $R/R_a$  of 6.81, an  $R_c/R_a$  of 10.30, and an  $F(^4\text{He})$  of 1.434. Lāna‘i well 1 has an  $R/R_a$  of 1.35, an  $R_c/R_a$  of 1.53, and an  $F(^4\text{He})$  of 0.481. Lāna‘i well 2 has an  $R/R_a$  of 0.84, an  $R_c/R_a$  of 0.76, and an  $F(^4\text{He})$  of 1.417. Lāna‘i well 14 has an  $R/R_a$  of 0.37, an  $R_c/R_a$  of 0.20, and an  $F(^4\text{He})$  of 0.335. These are the most diverse set of values from my study for any Hawaiian Island.

### **3.6 Maui**

Maui samples from the Ormat Technologies Inc. sampling campaign come from the southwest area of Haleakalā. The Wailea well has an  $R/R_a$  of 7.03, an  $R_c/R_a$  of 7.63, and an  $F(^4\text{He})$  of 4.02. The Horse well, which is on the southwest rift axis, but also very near sea-level, has an  $R/R_a$  of 2.93, an  $R_c/R_a$  of 3.15, and an  $F(^4\text{He})$  of 3.56.

### **3.7 Hawai‘i**

Because the island of Hawai‘i has multiple volcanoes at different volcanic stages, I have separated the data for this island by volcano or area.

#### **3.7.1 Kīlauea**

Ormat Technologies Inc. data from production wells at PGV on the East Rift of Kīlauea shows  $R/R_a$  values of 13.73 to 14.42,  $R_c/R_a$  up to 15.13, and  $F(^4\text{He})$  from 6.93 to 8.97. The USGS Hawaiian Volcano Observatory provided data from the Sulfur Banks fumaroles at the Kīlauea summit caldera show  $R/R_a$  13.41 to 15.56,  $R_c/R_a$  of up to 15.78, and  $F(^4\text{He})$  of 32.45 to 120.39. Note that PGV production samples are separated steam, and the Sulfur Banks samples are fumarolic gas, not dissolved gas in water as all other samples are. PGV monitoring wells had substantially lower values, with  $R/R_a$  of 1.69 to 2.8,  $R_c/R_a$  of 5.28 to 10.81, and  $F(^4\text{He})$  of 0.59 to 0.61. The monitoring wells are on the site of the PGV geothermal system, but do not directly tap the high temperature resource. I collected two additional samples near PGV, but not on the rift

zone. The Pāhoa Deep well 2, ~2 km north of the rift axis, had an  $R/R_a$  of 1.6, and an  $F(^4\text{He})$  of 0.29. The Kalapana Deep well, ~2.5 km south of the rift axis, had an  $R/R_a$  of 1.11, and an  $F(^4\text{He})$  of 0.27. Neither off-rift sample was suitable for the  $R_c/R_a$  correction.

### **3.7.2 Mauna Loa**

I collected three samples from Mauna Loa. One sample, along the southwest rift zone at Hawaiian Ocean View Estates (HOVE) had an  $R/R_a$  of 2.58, and an  $F(^4\text{He})$  of 0.37. The remaining two samples were from the inactive Nīnole rift (Morgan et al. 2010, Zurek et al. 2015). The Na‘ālehu Deep Well has an  $R/R_a$  of 1.07, and an  $F(^4\text{He})$  of 0.26, and the Pāhala Deep Well has an  $R/R_a$  of 1.05, and an  $F(^4\text{He})$  of 0.26.

### **3.7.3 Hualālai**

The six samples from Hualālai are from the Ormat Technologies Inc. study. Wells HR-1, HR-4, and HR-5 were sampled at two different times, approximately 6 months apart. Variation in helium between those two periods was minimal. HR-1, HR-3, HR-4, and HR-5 have similar values to one another, with  $R/R_a$  of 6.54 to 8.67,  $R_c/R_a$  of 8.02 to 9.35, and  $F(^4\text{He})$  of 1.75 to 4.41. The four HR wells sit directly on Hualālai’s Northwest rift zone. The other two wells, Kalaoa and Hualālai, are off rift, 3 and 4.5 km respectively. Kalaoa well water has an  $R/R_a$  of 1.94, an  $R_c/R_a$  of 4.53, and an  $F(^4\text{He})$  of 0.47. Hualālai well water has an  $R/R_a$  of 2.16, an  $R_c/R_a$  of 4.47, and an  $F(^4\text{He})$  of 0.51. Both of these off-rift samples show dilution of mantle helium with ASW.

### **3.7.4 Waikoloa**

The Waikoloa area sits nearly centered between the volcanoes of Kohala, Mauna Kea, and Hualālai. I collected four samples from this area. The Waiki‘i Well, which is nearest to Mauna Kea, has water with an  $R/R_a$  of 1.4, and an  $F(^4\text{He})$  of 0.30. Pu‘u Lani, closest to Hualālai, has an  $R/R_a$  of 1.82, and an  $F(^4\text{He})$  of 0.29. DW-3 well is farthest from any of the aforementioned volcanoes, and is near the town of Waikoloa. DW-3 well water has an  $R/R_a$  of 1.00, and an  $F(^4\text{He})$  of 0.29. The Lalamilo C well is closest to Kohala, and its water has an  $R/R_a$  of 1.12, with an  $F(^4\text{He})$  of 0.28. The Kawaihae 3 well on the southern edge of Kohala was a prime target, with water temperature of 36°C at 305 m. I was unfortunately unable to sample this well.

## 4. Discussion

### 4.1 Statewide Overview

The results of my study clearly show that helium anomalies and heat sources in Hawai‘i exist away from active surface volcanism. Hawai‘i, with multiple active volcanoes, and East Maui, clearly show the greatest divergence in helium values from ASW, and the most potential for geothermal resource. Lāna‘i has helium anomalies, and warm waters in a number of wells within the Pālāwai Basin, giving a moderately high probability of a geothermal system there. Only a minor helium anomaly was recorded for O‘ahu well waters, though my sampling was limited. Additional sampling is needed on O‘ahu to fully assess any geothermal presence on the island. Kaua‘i, the oldest of the main Hawaiian Islands, showed higher than expected helium anomalies with associated warm waters, representing a potential resource within the Līhu‘e Basin. Except for one well on Maui, noble gas anomalies across all volcanoes are present exclusively in areas identified as rift zones or calderas, though not all wells inside those structural features have anomalies.

Dilution of water carrying noble gases that differ from ASW, will move towards ASW noble gas values, gradually for helium, but more quickly for the other noble gases based on their atmospheric abundances and solubility. Most of my samples show a substantial degree of this mixing. This is because the majority of my well water samples are not directly located on a geothermal system, that is, a geothermal well would be quite noticeable and unlikely to go unreported. With few exceptions in my samples, and excluding helium, dilution with ASW has reduced all other noble gas anomalies (Ne, Ar, Kr, Xe) to ASW values, leaving only helium to trace thermal influence. Since end member reservoir  $F(^4\text{He})$  is not precisely known, I cannot provide a definite mixing proportion between ASW and these He reservoirs.

Figure 8 is a compilation of water dissolved or vapor carried helium volume ( $[\text{He}]$  cc/g) and  $R/R_a$  for Hawai‘i from this study and others, and data from Iceland for comparison. Three mixing lines between ASW with upper mantle, plume, and crust are plotted. Most of my results (open circles) fall between plume and upper mantle, as do most of the Ormat data, together forming a curvilinear trend ending at the samples from PGV. Notably, Lō‘ihi does not follow the rest of the Hawaiian trend, reaching higher  $R/R_a$  values, which is the result of being at the plume front yielding higher  $R/R_a$  and helium volume. Wells from Maui, O‘ahu, and Lāna‘i show a mixing

trend between ASW and a crustal component ( $R/R_a < 0.98$ ). Helium from Iceland shows ASW mixing with mantle plume, ASW mixing with upper mantle, and upper mantle and plume mixing together. This is expected as Iceland is fed magma from a mid-ocean ridge, as well as a mantle plume. Compared to the samples collected for this study, the Iceland data shown, while having a large spread, appears to indicate more simplistic mixing as no oceanic crustal component is evident. This is again as expected for at least some regions of Iceland. Given that it sits directly over a ridge axis, the underlying oceanic crust has not had ample time to ingrow a volume of radiogenic  $^4\text{He}$  that can shift  $R/R_a$  to  $< 1$ . The oceanic lithosphere under the Hawaiian Islands is approximately 90 Ma, while the approximate age of the oldest oceanic crust under Iceland is 32 Ma (Müller et al. 2008), and much of it is younger. The type of plot in Figure 8 can mask effects unrelated to dilution, such as phase separation (Smith and Kennedy 1983), and dilution, but is good for showing correlations between mixing members.

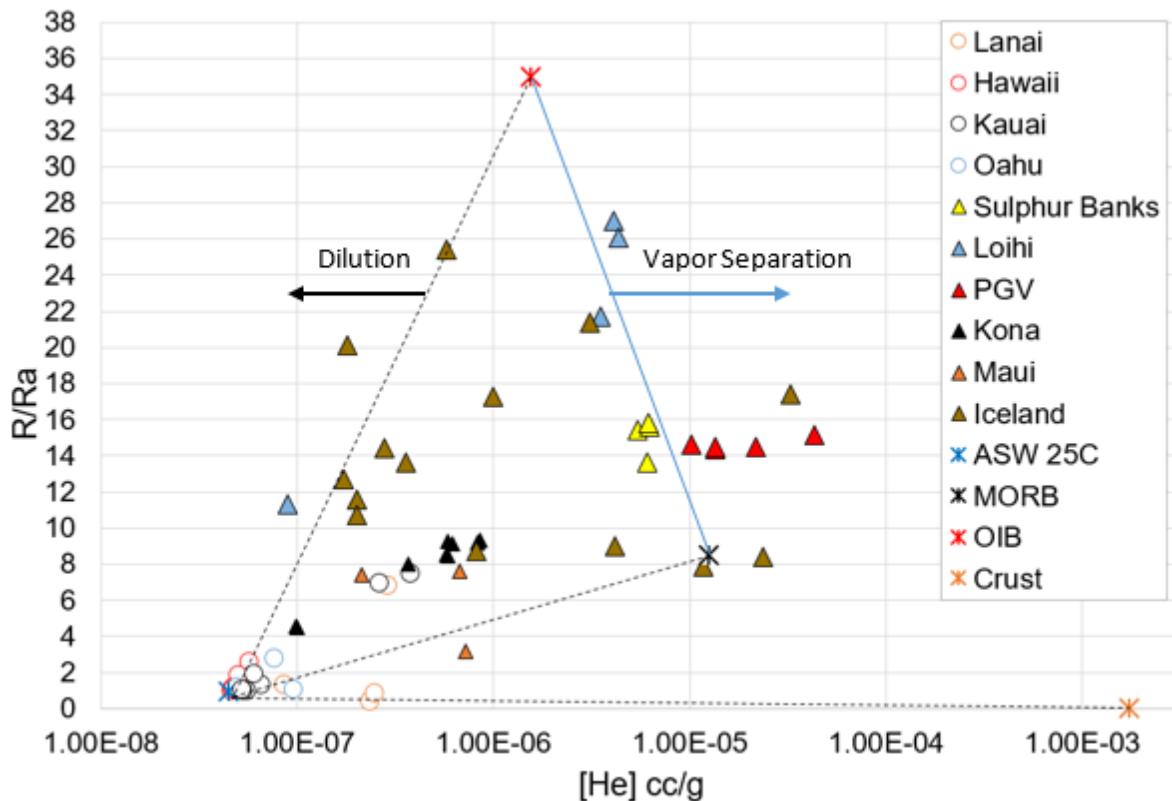


Figure 8. Plot of helium volume with  $R/R_a$ . Samples from this study are open circles, and reference studies are in filled triangles. Iceland samples are from Hilton et al. 1990 and Torgersen and Jenkins 1982. PGV, Kona, and Maui are from Fercho et al. 2015. Lō'ihi from Sedwick et al. 1994. End member values for ASW, plume and upper mantle (Ozima and Podosek

2004) and crust (mean of values, table 11: Ballentine and Burnard 2002) are symbolized as asterisks.

Stable isotopes  $^2\text{H}$  and  $^{18}\text{O}$  have been used to look for water-rock interaction as a means of identifying the presence of geothermal systems (Clark and Fritz 1997). Samples of water are compared to Vienna Standard Mean Ocean Water (VSMOW), in  $\delta\text{‰}$ -notation (McKinney et al. 1950).  $\delta^{18}\text{O}_{\text{VSMOW}}$  in geothermal settings may be off the meteoric water line (MWL) by 1 $\text{‰}$  to 20 $\text{‰}$  or more (Clark and Fritz 1997). Little in the way of shift off the local meteoric water line (LMWL) is seen in waters from this study (Figure 9), though samples from the Pōhakuloa Training Area (PTA, data provided by Donald Thomas, University of Hawai‘i) show a roughly a 1.5 $\text{‰}$  enrichment in  $\text{‰}^{18}\text{O}$  from the LMWL.

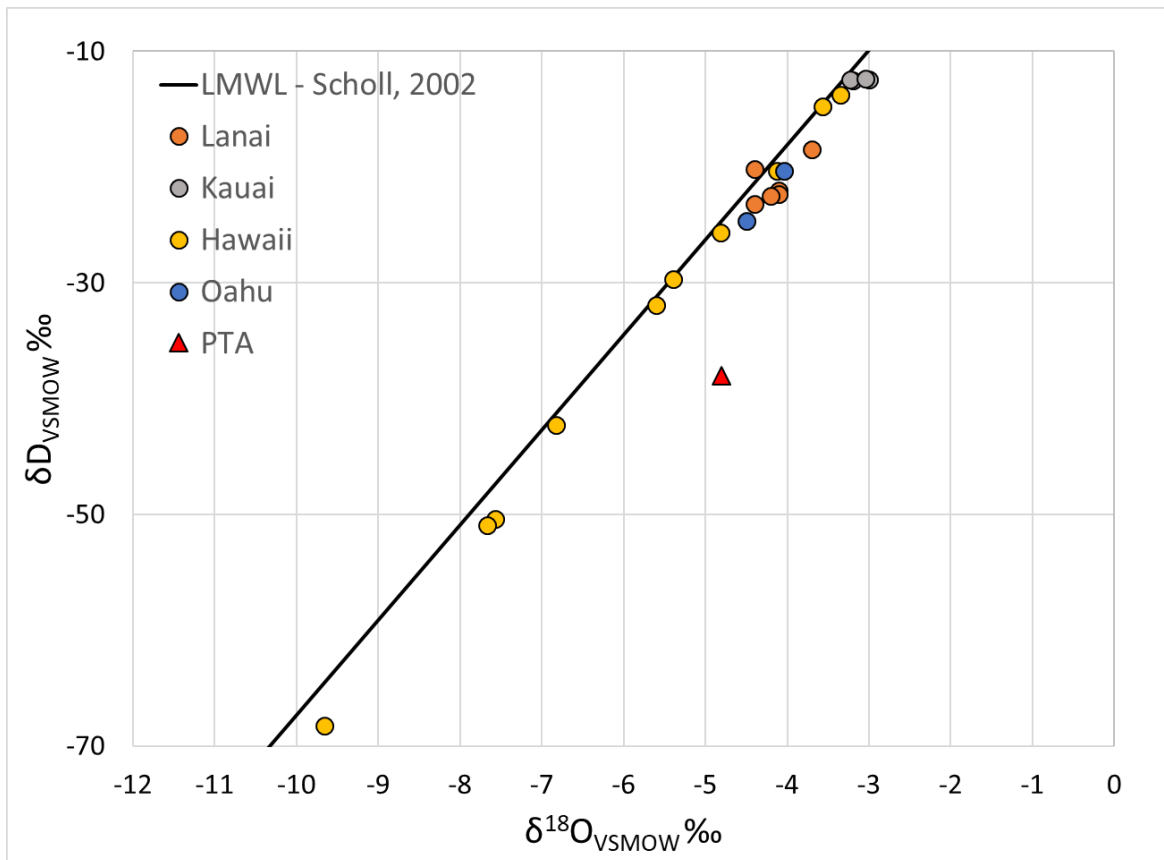


Figure 9. Isotope plot of water stable isotopes compared to the Local Meteoric Water Line (LMWL) of Scholl et al. 2002. The only sample that shows substantial water-rock interaction is from the Pōhakuloa Training Area (PTA, red triangle), with a shift in  $\delta^{18}\text{O}_{\text{VSMOW}}$  of 1.5 $\text{‰}$ . PTA sample data courtesy of Donald Thomas.

Mixing lines of ASW with crustal, mantle, and plume sources of helium are used to determine what noble gas reservoirs are contributing He to various well waters, as well as relative dilution with ASW. My data indicate that crustal components appear in a number of wells on multiple islands, but only on Lāna‘i are there wells that have predominantly crustal, radiogenic helium  $R/R_a$  values. The mantle-plume signal is most obvious in water from Hawai‘i island, but only at Kīlauea. The majority of samples across all islands show helium sourced from an upper mantle-like reservoir. Figure 10 shows the end member reservoirs, mixing lines, wells sampled in this study. Figure 11 is a close-up of Figure 10 for values near ASW. These two figures show that any helium anomaly in Hawai‘i can be a mixture of 5 components: Crust (oceanic lithosphere), ASW, upper mantle, plume, and small volumes of tritiogenic  $^3\text{He}$ . However, most samples can be described by two or three component mixing.

Because there is not a known helium reservoir with  $R/R_a$  between 1 (ASW) and 6.5 (upper mantle), most of the samples seen in Figure 11 are likely due to mixing between upper mantle and crustal sources, with dilution by ASW. It is possible that highly dilute plume helium is also mixing in these samples, but this cannot be separated from upper mantle helium at the low  $R/R_a$  values in Figure 11. Mixing of these two reservoirs causes a sample to fall off its mixing line between ASW and its upper mantle-like source reservoir, diagonally towards the crustal source, as increasing  $^4\text{He}$  volume increases  $F(^4\text{He})$  while decreasing  $R/R_a$ . Tritiogenic  $^3\text{He}$  would cause a water sample to move vertically away from ASW as it is only increasing  $^3\text{He}$  volume. This effect is not seen in this study. Tritiogenic  $^3\text{He}$  must be present, as tritium is present in all meteoric water, but it either can't be separated from other sources of  $^3\text{He}$ , or is of a very small volume.

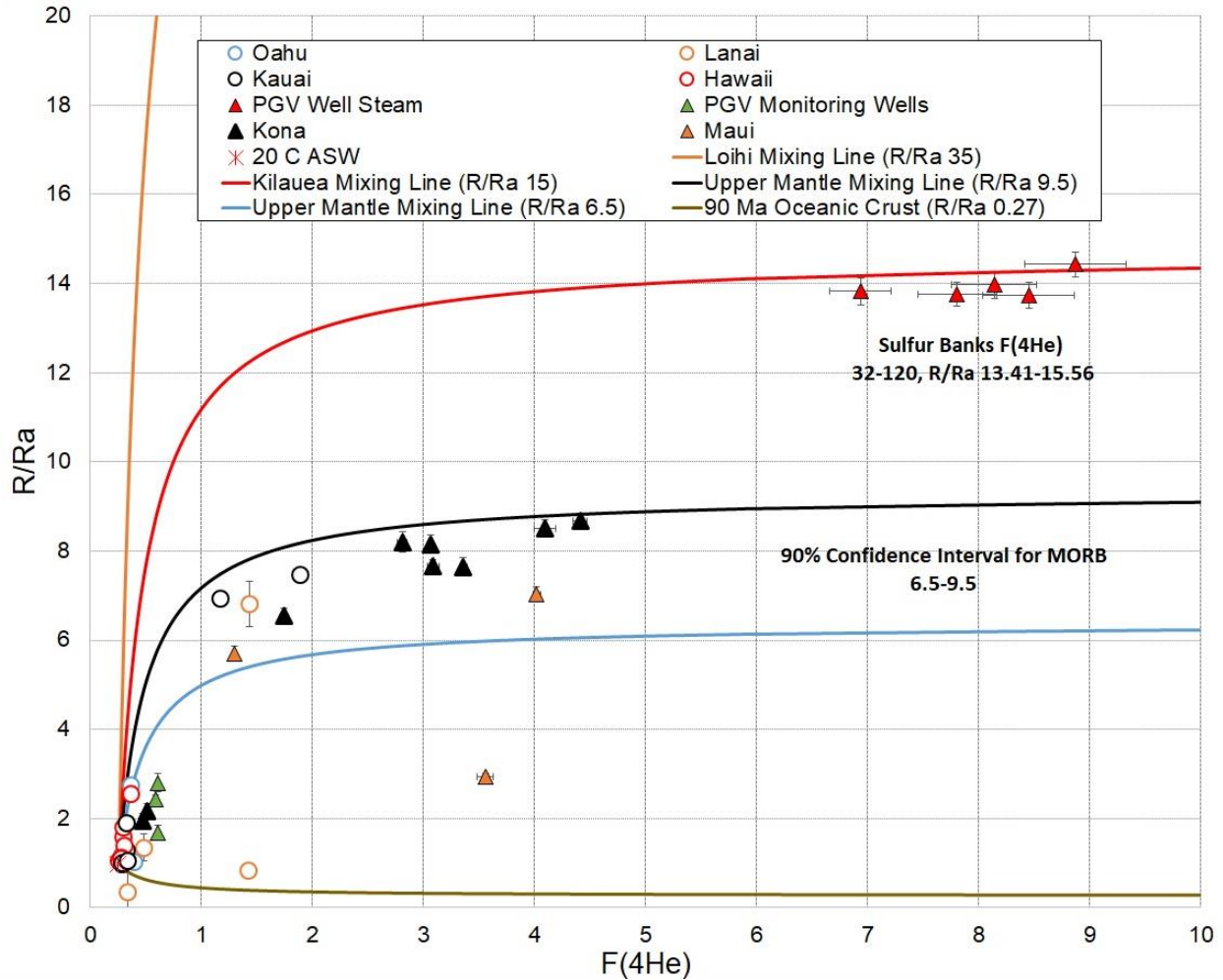


Figure 10. Mixing lines between ASW and end-member reservoirs. Reservoirs are inferred choices seen in this projects data. Many error bars are too small to be seen here, but can be found in the supplemental file. Filled triangles are data from Ormat Technologies Inc. or from the USGS. Open circles are new data from this study. The data from Sulphur Banks is well off this plot, because their  $F(^4\text{He})$  is at least 32, however, it is on the 15  $R/R_a$  mixing line. Most wells fall near ASW, mixing with an upper mantle-like source. A crustal, radiogenic source is evident as a mixing member and as a primary source. The 90% confidence interval for the upper mantle, listed here as MORB, is given by Graham 2002.

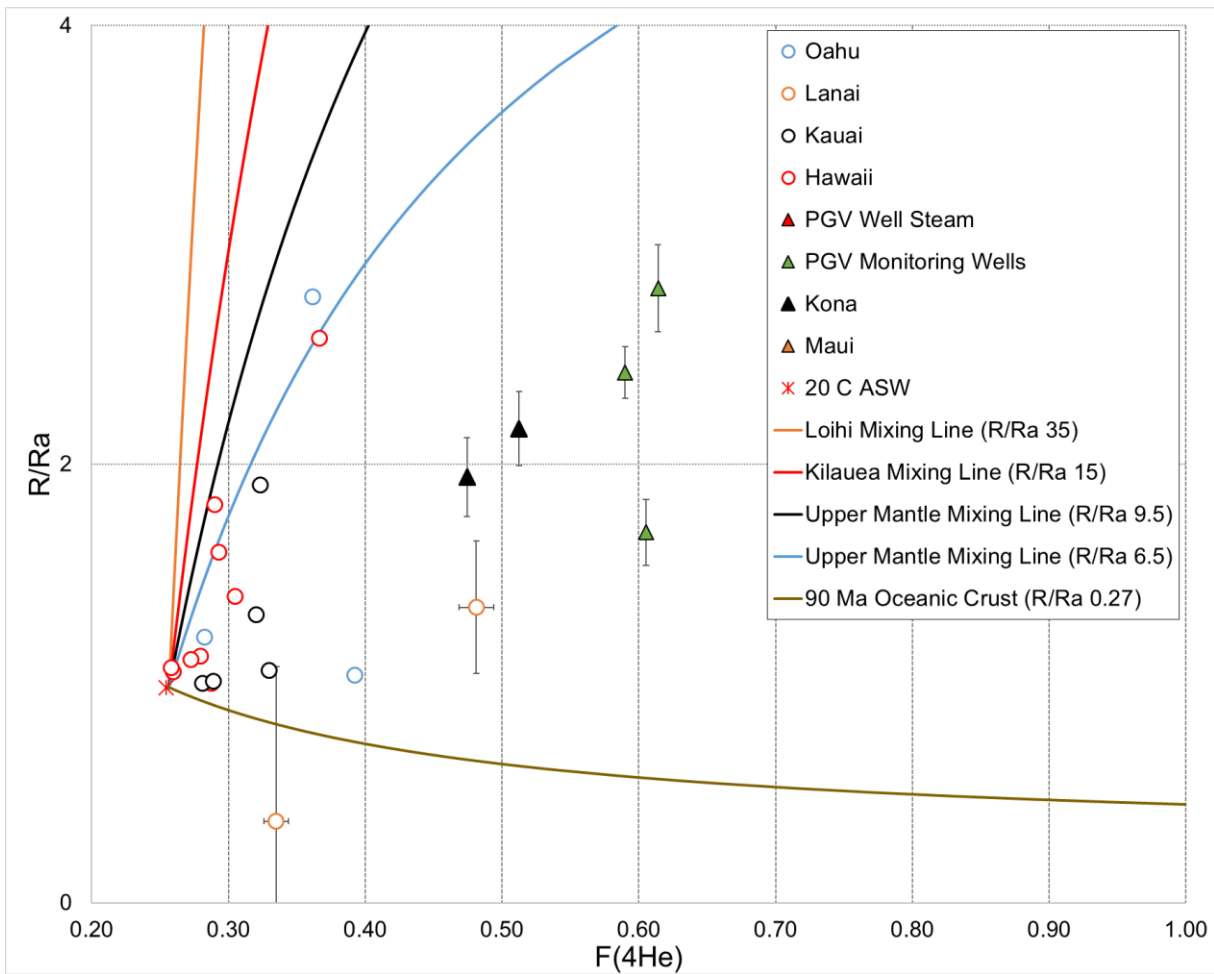


Figure 11. A view of Figure 11 focusing on helium values near ASW. Error bars are smaller than symbols where error is sufficiently low.

#### 4.1.1 Kaua‘i

The island of Kaua‘i is the oldest of the Hawaiian Islands sampled in this study. The Līhu‘e Basin (Figure 12) is one of the most prominent features of the island, and all of my samples are from within or near Līhu‘e Basin. A large gravity anomaly under the northern portion of Līhu‘e Basin and the interpretation of that gravity anomaly as a caldera (Holcomb et al. 1997, Flinders et al. 2009), the large rejuvenation volcanic center of Kilohana Crater inside the basin, the presence of warm groundwater (Lautze et al. 2020), and the presence of alteration minerals in core logs (Izuka and Gingerich 1997), all motivated sampling in this area, because all are indicators of a geothermal presence. The Hanamaulu well and Kilohana A well show an upper

mantle-like signal, with R/R<sub>a</sub> of ~7-7.5. At Hanamaulu an R<sub>c</sub>/R<sub>a</sub> of 9.49 puts this sample at the highest edge of upper mantle signal. These values are similar to those seen at Hualālai, and strongly suggest the presence of an active geothermal system. Geothermal resource in Līhu‘e therefore seems very likely. Studies of additional water samples from observation wells, as well as geophysical surveys using methods such as magnetotellurics are warranted.

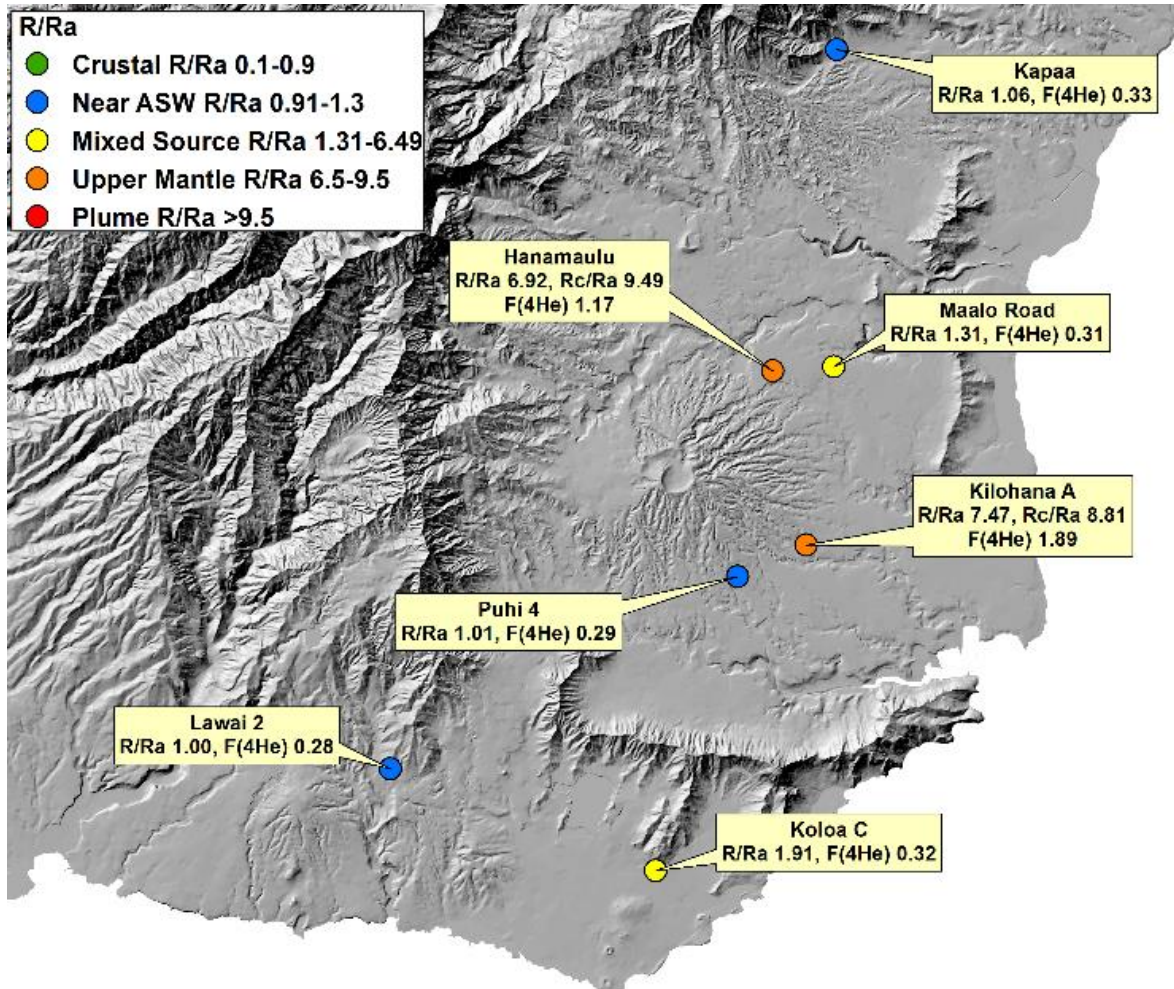


Figure 12. The Līhu‘e Basin of Kaua‘i. Kilohana Crater, a rejuvenation volcanism eruptive center, is a dominant feature inside the basin. Helium anomalies are in conjunction with Kilohana Crater, and in the south with a small chain of rejuvenation volcanic cones. Wells are symbolized by R/R<sub>a</sub> value for the well as matched to known helium reservoir R/R<sub>a</sub> values.

#### 4.1.2 O‘ahu

Of the three samples I collected on O‘ahu, all within the boundaries of mapped calderas (Figure 13), only the sample from the Royal Hawaiian Golf Course Well 4 (RHGC 4) showed any divergence from ASW with respect to  $R/R_a$ . Soil mercury maps (Cox et al. 1982, Thomas 1986) show elevated levels in the RHGC 4 area, which were used in those studies to show geothermal potential. Additionally, a fossil geothermal system is evident at RHGC 4 from rock samples I collected showing extensive alteration (Figure 14). Both RHGC 4 and the Sherill well held excess helium as seen in their  $F(^4\text{He})$ . RHGC 4 plots on an upper mantle-like mixing line, while Sherill Well plots below an upper mantle mixing line, indicating contribution from a crustal source of  $^4\text{He}$ . Lualualei well shows ASW  $F(^4\text{He})$ , but a slightly enriched  $R/R_a$ , suggesting the addition of tritiogenic  $^3\text{He}$ . The ASW-upper mantle mixing at RHGC 4 suggests that heat is present. More sampling within rift zones and calderas is needed.

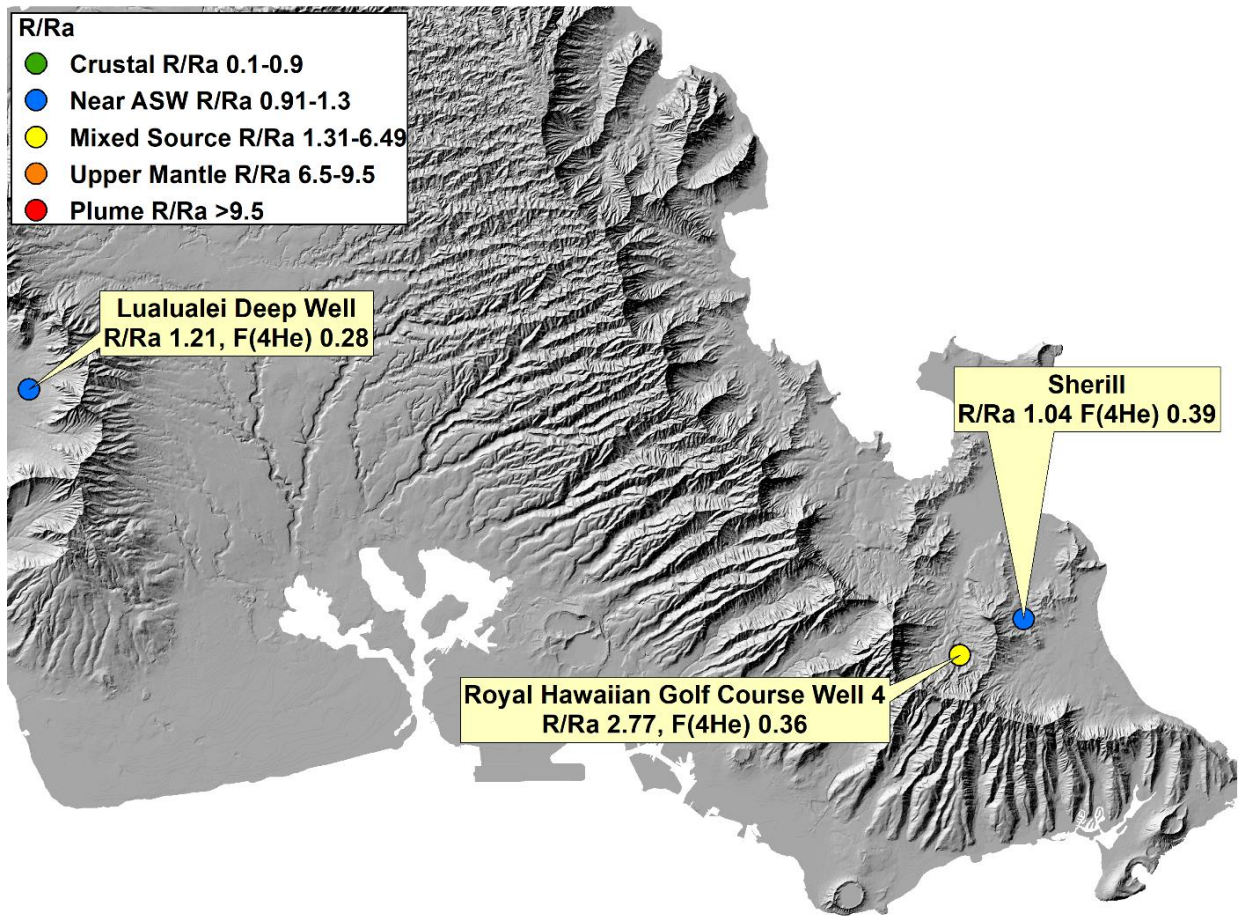


Figure 13. Samples from the island of O‘ahu. Wells are symbolized by R/R<sub>a</sub> value for the well as matched to known helium reservoir R/R<sub>a</sub> values.



Figure 12. Alteration minerals in a vug from the area around RHGC 4, including quartz and epidote, which indicate a fossil geothermal system with temperatures of at least 200°C (Reyes 1990). Additional photos are in the supplemental materials. The sample shown above has been fully altered from the original basalt, to an epidosite. Field of view approximately 3mm.

### 4.1.3 Lānaʻi

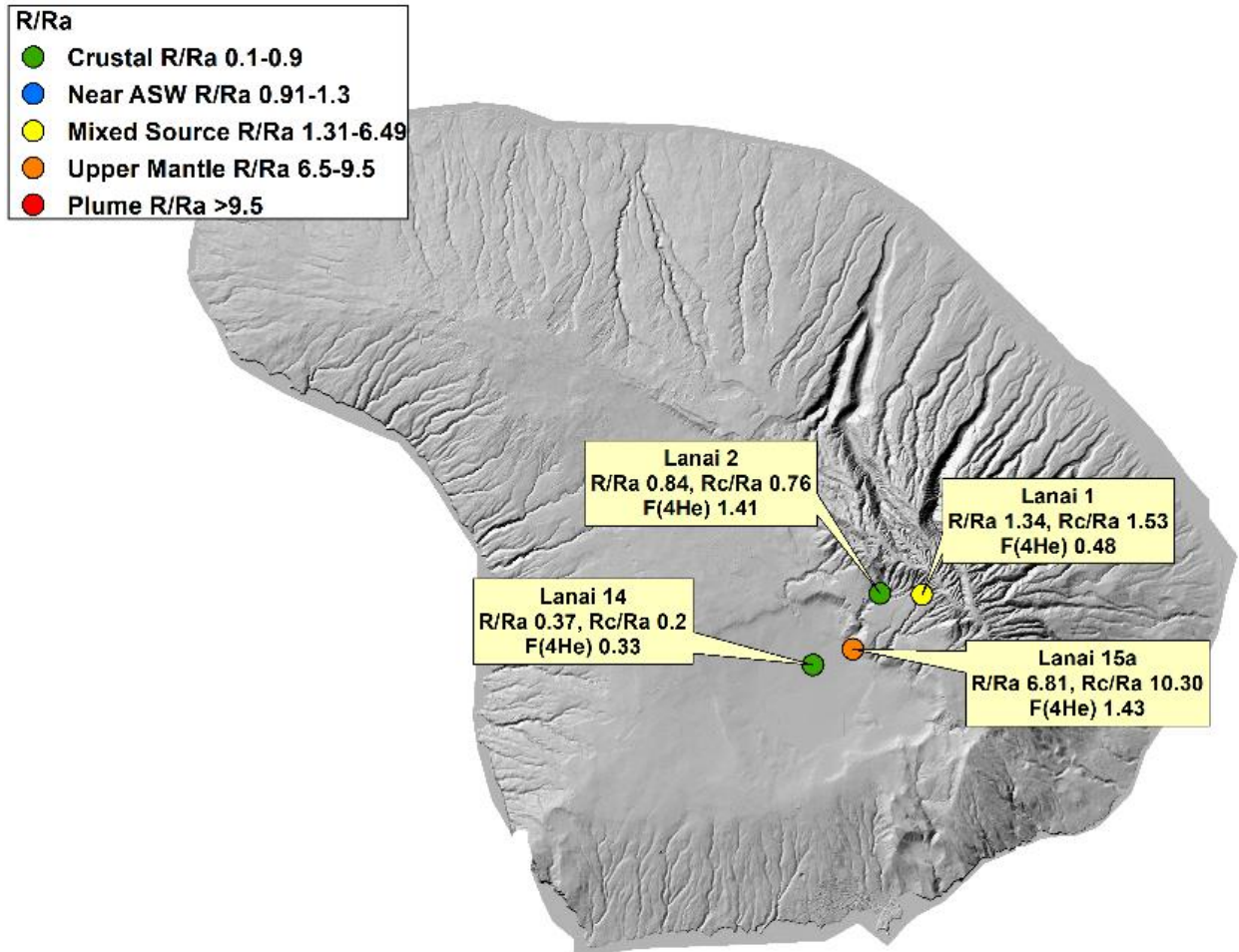


Figure 13. The island of Lānaʻi, the caldera of Pālāwai Basin, and the Northwest rift zone extending from the NE corner of the caldera. Wells are symbolized by R/R<sub>a</sub> value for the well as matched to known helium reservoir R/R<sub>a</sub> values.

Lānaʻi is thought to be an extinct volcano, which never proceeded past its shield building stage (West et al. 1992). However, there is warm, brackish water within the Palawai basin, at least high as 150 m.a.s.l. (Lautze et al. 2020) suggesting that some degree of heat remains in Lānaʻi. Brackish water high above sea level is likely due to a thermal convective cell, allowing buoyant rise of geothermal water (Figure 4). Lānaʻi well 10, from which I did not get a sample as it has no pump, has a bottom hole temperature of 43°C. Lānaʻi well 13, which is sealed at present, was reported to have bottom hole temperatures of 45°C (Lautze et al. 2017a). Lānaʻi well 2 has an

$R/R_a$  of 0.84, and an  $R_c/R_a$  of 0.76, while Lāna‘i well 14 has an  $R/R_a$  of 0.37 and an  $R_c/R_a$  of 0.2. Lāna‘i wells 2 and 14 are dominated by a radiogenic crustal source of helium (Figure 15). The ingrown  $^4\text{He}$  in my model of aged oceanic crust reduced the initial upper mantle value of  $R/R_a$  8 to  $R/R_a$  of 0.27, which is very close to the values found in wells 2 and 14. However, spatially close to wells 2 and 14, Lāna‘i well 15a has an  $R/R_a$  of 6.81 and an  $R_c/R_a$  of 10.30, which is above upper mantle values, representing a plume component. Lāna‘i must have a heat source as deep as the oceanic lithosphere in order to gain its  $R/R_a$  values of  $<1$ , and either connectivity to the mantle or an emplaced magma separate from the crustal heat source for upper mantle-plume  $R/R_a$ . Helium data alone cannot differentiate between these possibilities. Lāna‘i has high potential for a geothermal resource. Data complementary to this study have been produced and interpreted (Lautze et al. 2020). Additional exploratory drilling would quantify the maximum temperature of a resource.

#### **4.1.4 Maui – Haleakalā**

Haleakalā is an active, post-shield phase volcano. All data for Haleakalā are from an Ormat geothermal study (Fercho et al. 2015), and were collected on the Southwest rift zone of the volcano (Figure 16). All three wells on Maui show a dilute upper mantle signal. The Horse well shows a significant contribution from a crustal source in addition to the upper mantle, as can be seen in Figures 10 and 11, with the  $R/R_a$  plotting below an upper mantle mixing line, with an increased  $F(^4\text{He})$ . Interestingly, the two Wailea wells are the only wells throughout the Hawaiian Islands in my study that are not located on or near a rift zone or in a caldera, yet they have high  $R/R_a$  values. It is likely that the fluids in the Wailea wells originated in the Southwest Rift Zone of Haleakalā, and migrated northward through a highly permeable aquifer. A resource is clearly present in Haleakalā as evidenced by the helium anomalies in well water and the presence of young volcanism (Sherrod et al. 2006).

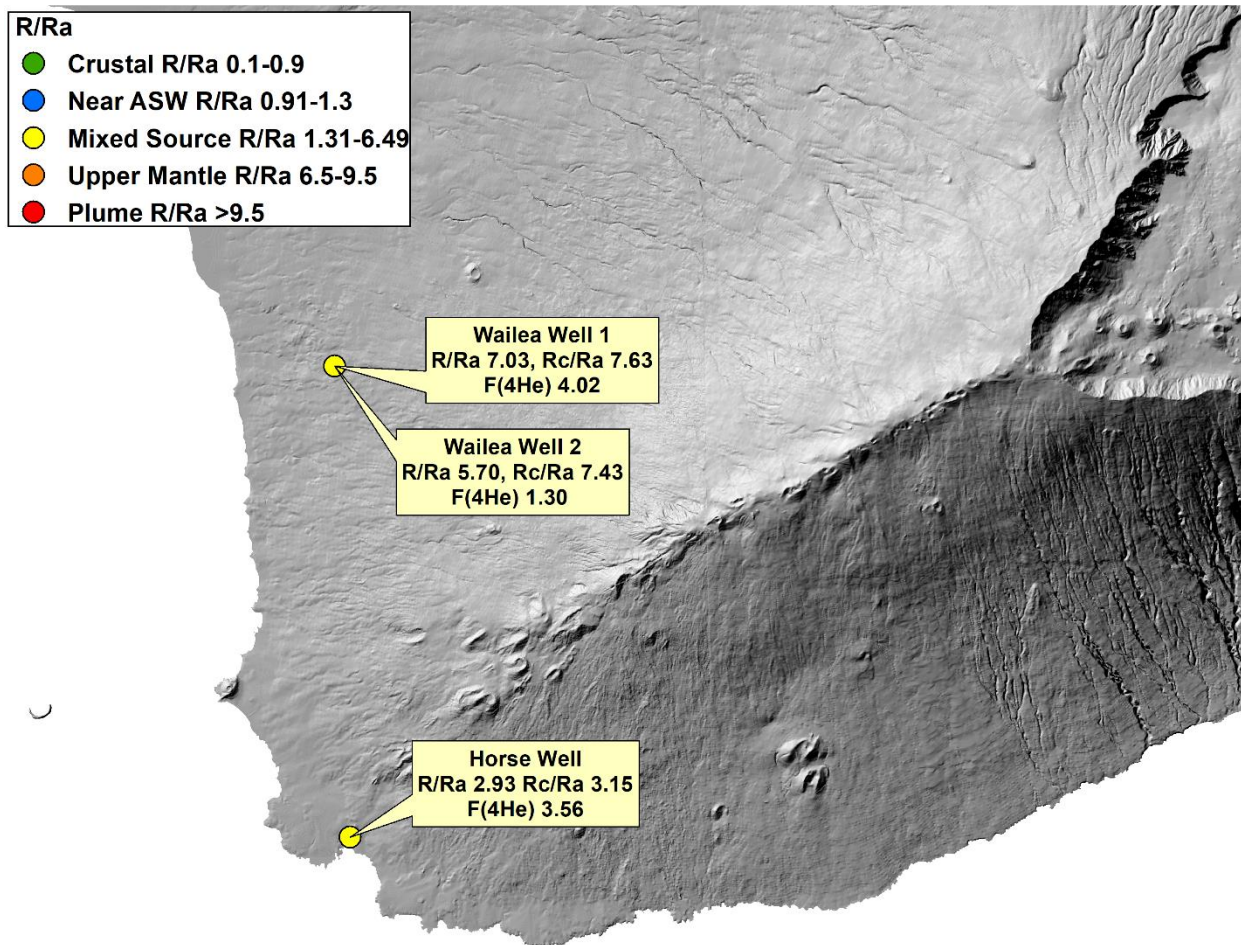


Figure 14. Southwest rift zone of Haleakalā on the island of Maui, and the three wells sampled by Ormat. All have strong helium anomalies, revealing the presence of a geothermal resource. Wells are symbolized by R/R<sub>a</sub> value for the well as matched to known helium reservoir R/R<sub>a</sub> values.

#### 4.1.5 Hawai‘i - Hualālai and Waikoloa

At the active volcano Hualālai, Ormat (Fercho et al. 2015) sampled 8 wells, both directly on, and off rift. Overall, Hualālai shows very clear helium from an upper mantle-like source (Figure 17). The helium anomaly is far stronger directly on rift, though a lower helium anomaly is present in the off-rift samples. The helium anomalies at Hualālai show a geothermal system is present within the rift system, and/or possibly below the summit. The Pu‘u Lani well sits in the Pu‘u Anahulu trachyte flow, which originates from the Pu‘u Wa‘awa‘a cone on the northern flank of Hualālai. Pu‘u Wa‘awa‘a has been the site of prior geothermal investigation, though no

economic resource was found (Thomas 1986). However, a small helium anomaly exists, suggesting a weak source is still present near Pu‘u Wa‘awa‘a, as sampled from the Pu‘u Lani well. The Waikoloa area wells show low helium anomalies, with  $F(^4\text{He})$  at ASW value, suggesting the addition of tritiogenic  $^3\text{He}$  as the cause of the slightly higher  $R/R_a$ . No resource is apparent in the Waikoloa area from my data, however, I was unable to sample the Kawaihae 3 well, which was previously identified as in a possible geothermal resource area based in well temperature and chemistry (Thomas 1986).

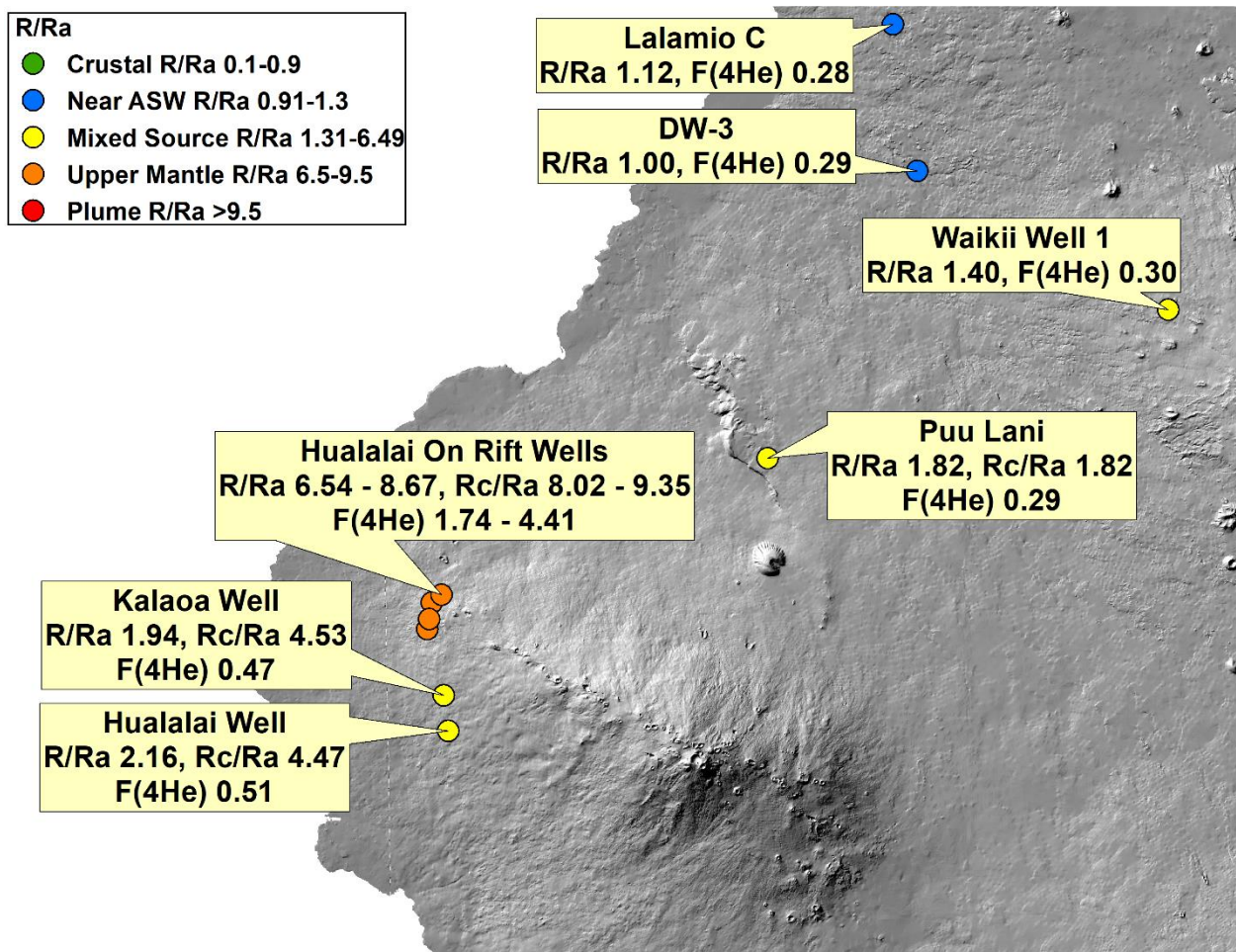


Figure 15. Hualālai and Waikoloa area samples. Hualālai shows upper mantle helium anomalies, while Waikoloa samples show anomalies I interpret as tritiogenic  $^3\text{He}$ . Wells are symbolized by  $R/R_a$  value for the well as matched to known helium reservoir  $R/R_a$  values.

#### **4.1.6 Hawai‘i - Kīlauea and Mauna Loa**

Mauna Loa is an active, shield building volcano. I sampled two wells from the abandoned (extinct) Nīnole rift (Morgan et al. 2010), from the Pāhala deep well, and the Nā‘ālehu well. Neither of these wells show notable helium anomalies. Despite the dense network of fractures in the area (Sherrod et al. 2007), and proximity to the Southwest Rift of Mauna Loa, these wells are not interacting with a heat source or degassing volatiles. The Hawaiian Ocean View Estates well (HOVE) shows a dilute upper mantle helium signal, falling on a mixing line between  $R/R_a$  6.5 and ASW. This upper mantle mixing line closely matches the average  $R/R_a$  of recent volcanic activity of Mauna Loa, as shown in core analysis from the Hawai‘i Scientific Drilling Project (DePaolo et al. 2001). Despite being the closest subaerial volcano to Kīlauea, Mauna Loa shows a reduction in the plume helium signal, in its youngest volcanic rocks, just as Kīlauea does from Lō‘ihi. HOVE is slightly off rift (Figure 18), which is the probable cause of diluted  $R/R_a$  despite being on an active volcano. Unsurprisingly, a heat source, possibly weak at present, lies within the active Southwest Rift Zone of Mauna Loa.

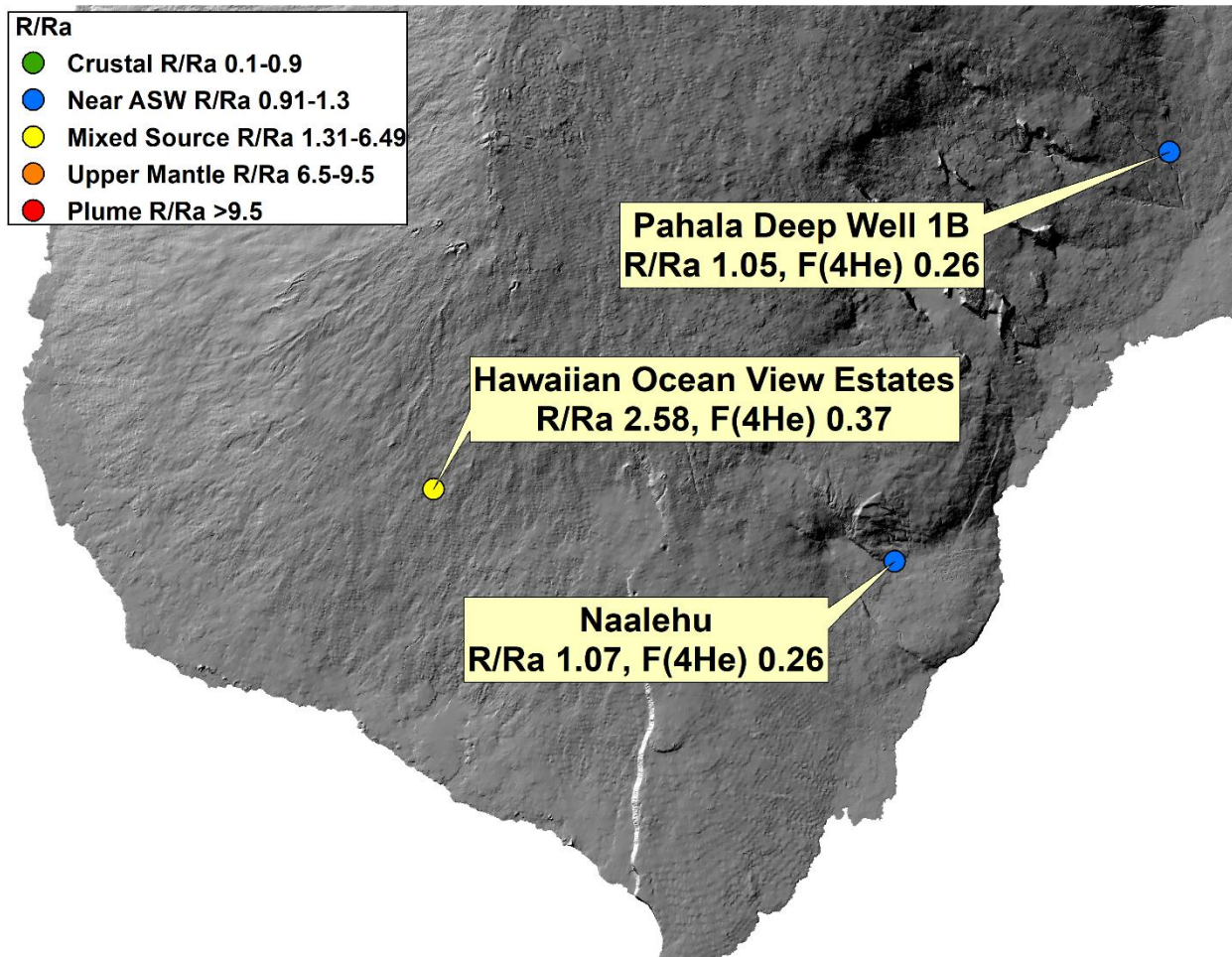


Figure 16. Samples from Mauna Loa. The upper mantle signal at HOVE suggests a resource, though potentially weak. Wells are symbolized by  $R/R_a$  value for the well as matched to known helium reservoir  $R/R_a$  values.

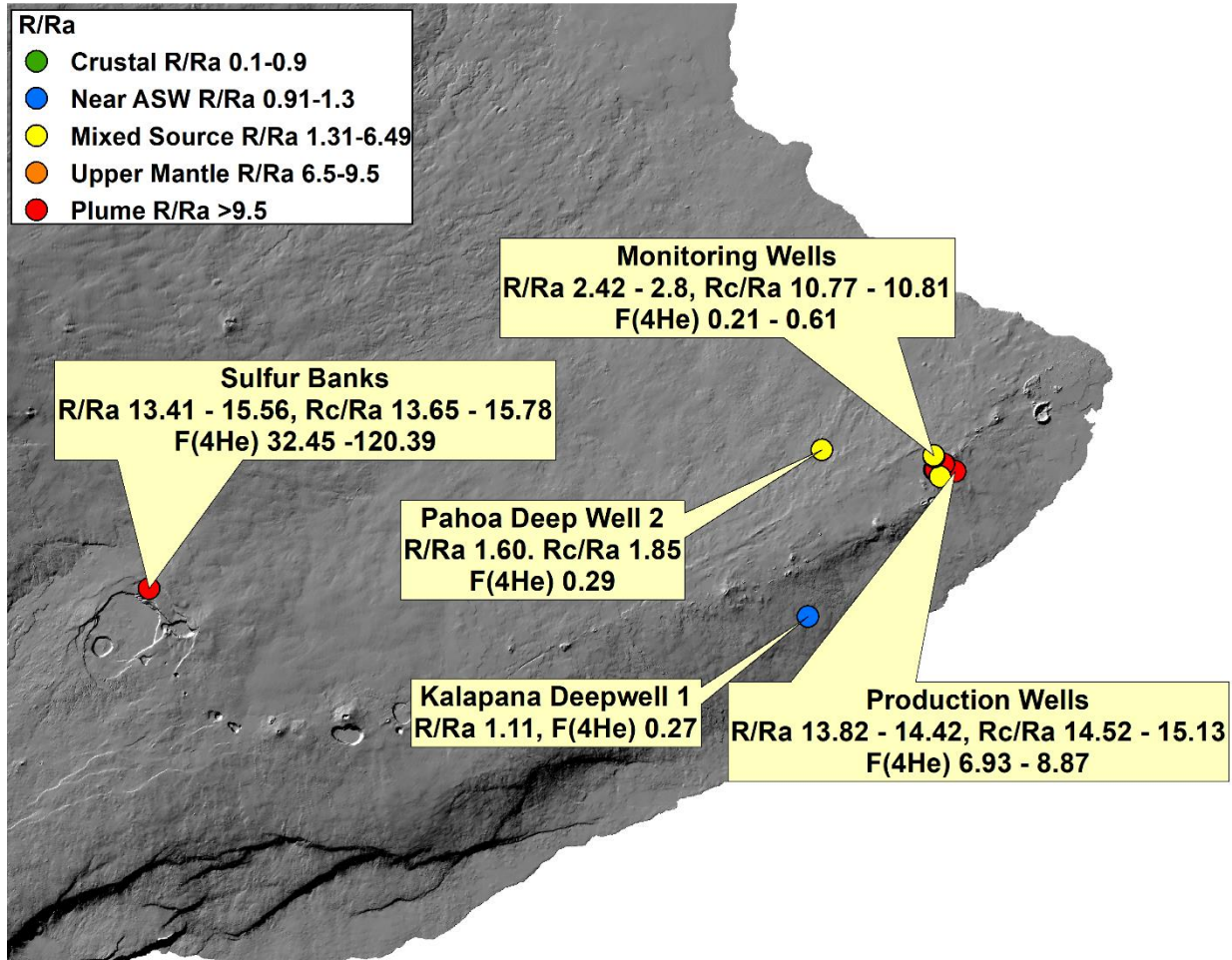


Figure 19. Samples from the Sulphur Banks, off-rift near PGV, and at PGV for monitoring and production wells. The off-rift samples show how dilution of a primary signal can happen over a short space. The samples from the Sulphur banks and PGV bear striking similarity, as they are fed by the same deep magma chamber (Ep et al. 1982, Neal et al. 2018). Wells are symbolized by  $R/R_a$  value for the well as matched to known helium reservoir  $R/R_a$  values.

With high rates of active volcanism and proximity to the mantle-plume core, it is not surprising that Kīlauea and its East Rift Zone (KERZ) show very strong mantle-plume helium anomalies in waters, steam, and volcanic rocks (Figure 19). Other than Lō‘ihi seamount, this area has the highest  $R/R_a$  for fluids, vapors, and recent lavas. At depth the Sulphur Banks fumaroles and PGV are both connected to the same primary magma chamber from the plume (at depth), and the

strong helium anomaly present in both locations exemplifies the relationship between helium and heat.

#### **4.2 Mantle Helium Trends Along the Main Hawaiian Chain**

Prior studies have looked at  $R/R_a$  trends through the lifespan of individual Hawaiian volcanoes and found that as a volcano reaches its final stages of activity, the  $R/R_a$  gradually drops from its plume highs to upper mantle values of around 8 (Kurz and Kammer 1991, DePaolo et al. 2001, Hoffman et al. 2011). Whereas there is variability at each volcano in  $R/R_a$  over time, the overall trend is towards the upper mantle  $R/R_a$ , as a volcano moves away from the plume and grows older. This pattern holds for each volcano. Degassing of noble gases through dissolution into other volatiles, such as  $\text{CO}_2$ , may account for some of this loss. However, if degassing of the plume is a continuous process, there is no reason for the  $R/R_a$  to consistently stop at an  $R/R_a$  of approximately 8, and there must be some other process that keeps the  $R/R_a$  of both waters and rocks from dropping below 8. One such process would be transport of upper mantle helium by a low melting temperature, low viscosity melt as a possible cause for the  $R/R_a$  8 values at the surface. Low viscosity melts can easily acquire helium from their surroundings, and can migrate through the upper mantle (Hofman et al. 2011). As an island ages and moves farther away from the plume front, any entrained melts will interact with the upper mantle. As the upper mantle is far more voluminous than any plume melts, a residual melt component will be interacting with an effectively infinite volume of helium at  $R/R_a$  8, and thus take on that value. Using the plume model of Ribe and Christensen (1999), improved upon by Farnetani and Hofman (2010), and incorporating the low viscosity flow model of Hofman et al. (2011), it is possible to provide a mechanism for residual low viscosity melts, either trapped in the oceanic crust, or in the upper mantle to be reactivated and contribute their helium to fluids and magmas of late-shield, alkali, and rejuvenation volcanics. As this study has focused on helium alone, I cannot propose a composition for the suggested melt phase.

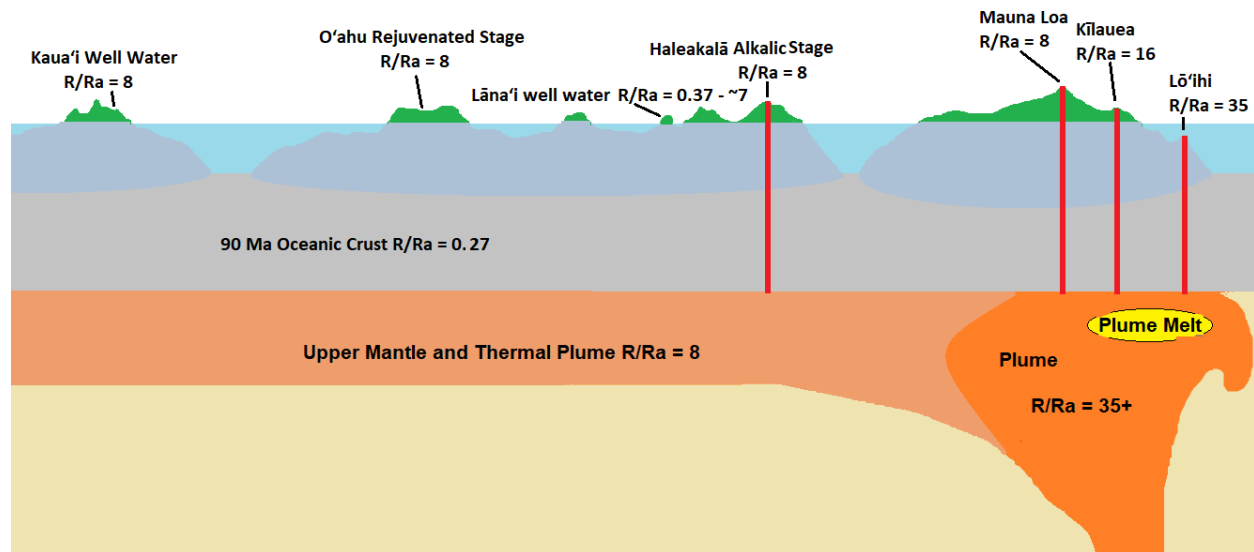


Figure 17. Cross section of the Hawaiian Islands from southeast (right) to northwest (left) and the underlying crust, upper mantle, and plume, showing the  $R/R_a$  of each noble gas reservoir, and the  $R/R_a$  for the rocks from youngest volcanism or current well waters for select volcanoes or islands. A rapid progression in  $R/R_a$  towards that of the upper mantle happens over short distance, and is present in the thermal plume (residual plume heat and melts) by partitioning of noble gases from the upper mantle into a low viscosity melt. Base layer cross section adapted from Simkin et al. (2006)

## 5. Conclusions

This study is a part of the Hawai‘i Play Fairway Analysis, Phase 3, and is based on the results from the first two phases. Analysis of helium dissolved in groundwater is an effective early geothermal exploration tool, that is less affected by dilution and transport of geothermal waters than the other tracers used in this study. On all islands in this study mantle helium is present in some, though not all, groundwater, indicating potential geothermal resources of unknown economic value as helium alone cannot be used as a geothermometer. Helium anomalies, and thus geothermal heat potential, appear restricted to wells located on rifts or in calderas, with the exception of one well on Maui that is likely fed by water discharging from a rift. The drop in  $R/R_a$  from plume to upper mantle-like values is likely the result of partitioning of upper mantle helium into a residual low viscosity melt phase produced by the plume. A reduction in  $R/R_a$  alone indicates a higher level of dilution with ASW, and not necessarily a reduction in the vigor of a resource, as an upper mantle-like  $R/R_a$  is seen in late shield building through rejuvenation volcanism throughout the Hawaiian Islands. A reduction in  $R/R_a$  coupled with an increase in  $F(^4\text{He})$  indicates the incorporation of an aged oceanic crustal helium component, as is modeled for the 90 Ma oceanic crust under the Hawaiian Islands. Tritogenic helium is present in some of the wells, but it makes a minor contribution to  $R/R_a$ . Mixing lines with inferred end member helium reservoirs are an effective way to understand the potential heat source  $R/R_a$ , mixing between helium reservoirs, and contribution from tritogenic helium. The results of this study show a high likelihood of a geothermal resource on the islands of Kaua‘i and Lāna‘i, as indicated by warm well waters and strong upper mantle-like helium anomalies, in addition to the known resources at active and recently dormant volcanoes. The experimental check-valve sampler proved that it could contain dissolved noble gases in excess of the atmosphere, though it should in the future be designed with an adjustable check-valve that can be set to a desired pressure to reach target depths in a well.

## References

- Aeschbach-Hertig W., and Solomon D.K. (2013). Noble Gas Thermometry in Groundwater Hydrology. In: Burnard P. (eds) *The Noble Gases as Geochemical Tracers. Advances in Isotope Geochemistry*. Springer, Berlin, Heidelberg. doi.org/10.1007/978-3-642-28836-4\_5
- Annen, C., and Sparks, R. (2002). Effects of Repetitive emplacement of basaltic intrusions on thermal evolution and melt generation in the crust. *Earth and Planetary Science Letters*, 203(3-4), pp937-955. doi.org/10.1016/s0012-821x(02)00929-9
- Arnórsson, S. (1978). Major element chemistry of the geothermal sea-water at Reykjanes and Svartsengi, Iceland. *Mineralogical Magazine*, 42(322), pp.209-220. doi:10.1180/minmag.1978.042.322.07
- Bach, W., Peucker-Ehrenbrink, B., Hart, S. and Blusztajn, J., (2003). Geochemistry of hydrothermally altered oceanic crust: DSDP/ODP Hole 504B - Implications for seawater-crust exchange budgets and Sr- and Pb-isotopic evolution of the mantle. *Geochemistry, Geophysics, Geosystems*, 4(3). doi.org/10.1029/2002GC000419
- Bach, W., Alt, J., Niu, Y., Humphris, S., Erzinger, J. and Dick, H., (2001). The geochemical consequences of late-stage low-grade alteration of lower ocean crust at the SW Indian Ridge: results from ODP Hole 735B (Leg 176). *Geochimica et Cosmochimica Acta*, 65(19), pp.3267-3287. doi.org/10.1016/S0016-7037(01)00677-9
- Ballentine, C. and Burnard, P., (2002). Production, Release and Transport of Noble Gases in the Continental Crust. *Reviews in Mineralogy and Geochemistry*, 47(1), pp.481-538. doi.org/10.2138/rmg.2002.47.12
- Berehannu, M., (2014). *Geochemical Interpretation Of Discharge From Reykjanes Wells RN-29 And RN-32, SW-Iceland*. United Nations University Geothermal Training Program. Reykjavik: United Nations University, pp.Reports 2014 Number 19.
- Carling, G., Radebaugh, J., Saito, T., Lorenz, R., Dangerfield, A., Tingey, D., Keith, J., South, J., Lopes, R. and Diniega, S., (2015). Temperatures, thermal structure, and behavior of eruptions at Kilauea and Erta Ale volcanoes using a consumer digital camcorder. *GeoResJ*, 5, pp.47-56. doi.org/10.1016/j.grj.2015.01.001
- Cashman, K., Thornber, C. and Kauahikaua, J., (1999). Cooling and crystallization of lava in open channels, and the transition of Pāhoehoe Lava to 'A'ā. *Bulletin of Volcanology*, 61(5), pp.306-323.
- Clark, I. and Fritz, P., (1997). *Environmental Isotopes In Hydrogeology*. Boca Raton: CRC Press.
- Coogan, L., Jenkin, G. and Wilson, R., (2007). Contrasting Cooling Rates in the Lower Oceanic Crust at Fast- and Slow-spreading Ridges Revealed by Geospeedometry. *Journal of Petrology*, 48(11), pp.2211-2231. doi.org/10.1093/petrology/egm057
- Cox, M., Cuff, K., Lienert, B., Sinton, J., and Thomas, D., (1982). *A Preliminary Geothermal Evaluation Of The Mokapu Peninsula On The Island Of Oahu, Hawaii*. Hawaii Institute of Geophysics Technical Report. HIG-82-2.

- Craig, H., Lupton, J., Welhan, J. and Poreda, R., (1978). Helium isotope ratios in Yellowstone and Lassen Park volcanic gases. *Geophysical Research Letters*, 5(11), pp.897-900. doi.org/10.1029/GL005i011p00897
- Crundwell, F., (2014). The mechanism of dissolution of forsterite, olivine and minerals of the orthosilicate group. *Hydrometallurgy*, 150, pp.68-82. doi.org/10.1016/j.hydromet.2014.09.006
- Cruz, J. and França, Z., (2006). Hydrogeochemistry of thermal and mineral water springs of the Azores archipelago (Portugal). *Journal of Volcanology and Geothermal Research*, 151(4), pp.382-398. doi.org/10.1016/j.jvolgeores.2005.09.001
- DePaolo, D., Bryce, J., Dodson, A., Shuster, D. and Kennedy, B., (2001). Isotopic evolution of Mauna Loa and the chemical structure of the Hawaiian plume. *Geochemistry, Geophysics, Geosystems*, 2(7). doi.org/10.1029/2000GC000139
- Ellis, E. (1827). *Journal of William Ellis – A Narrative of a Tour Through Hawaii in 1823*. Rutland: Charles E. Tuttle Company.
- Epp, D., Decker, R. and Okamura, A., (1983). Relation of summit deformation to East Rift Zone eruptions on Kilauea Volcano, Hawaii. *Geophysical Research Letters*, 10(7), pp.493-496. doi.org/10.1029/GL010i007p00493
- Evans, W., Bergfeld, D., Sutton, A., Lee, R. and Lorenson, T., (2015). Groundwater chemistry in the vicinity of the Puna Geothermal Venture Power Plant, Hawai‘i, after two decades of production. USGS Scientific Investigations Report 2015-5139. doi.org/10.3133/sir20155139
- Farnetani, C.G. and Hofmann, A.W. (2010). Dynamics and internal structure of the Hawaiian plume. *Earth and Planetary Science Letters*, 295(1–2), pp.231–240. doi.org/10.1016/j.epsl.2010.04.005
- Fercho, S., Owens, L., Walsh, P., Drakos, P., Martini, B., Lewicki, J.L. and Kennedy, B.M. (2015). Blind Geothermal System Exploration in Active Volcanic Environments; Multi-phase Geophysical and Geochemical Surveys in Overt and Subtle Volcanic Systems, Hawai‘i and Maui. USDOE Geothermal Technologies Office Technical Report, DE-EE0002837. doi.org/10.2172/1242411
- Flinders, A., Ito, G., and Garcia, M., (2010). Gravity anomalies of the Northern Hawaiian Islands: Implications on the shield evolutions of Kauai and Niihau, *J. Geophys. Res.*, 115. doi.org/10.1029/2009JB006877
- Flynn, L. and Mougini-Mark, P. (1992). Cooling rate of an active Hawaiian lava flow from nighttime spectroradiometer measurements. *Geophysical Research Letters*, 19(17), pp.1783–1786. doi.org/10.1029/92GL01577
- Fournier, R. and Potter, I. (1982). Revised and expanded silica (quartz) geothermometer. *Bull., Geotherm. Resour. Counc. (Davis, Calif.); (United States)*, [online] 11:10(November 1982). Available at: <http://pubs.geothermal-library.org/lib/grc/7000176.pdf> [Accessed 30 Oct. 2020].

Gamo, T., Chiba, H., Yamanaka, T., Okudaira, T., Hashimoto, J., Tsuchida, S., Ishibashi, J., Kataoka, S., Tsunogai, U., Okamura, K., Sano, Y. and Shinjo, R. (2001). Chemical characteristics of newly discovered black smoker fluids and associated hydrothermal plumes at the Rodriguez Triple Junction, Central Indian Ridge. *Earth and Planetary Science Letters*, 193(3–4), pp.371–379. doi.org/10.1016/S0012-821X(01)00511-8

Geothermex, (2000). UPDATE OF THE STATEWIDE GEOTHERMAL RESOURCE ASSESSMENT OF HAWAII for THE STATE OF HAWAII DEPARTMENT OF BUSINESS, ECONOMIC DEVELOPMENT AND TOURISM. (2000). [online] Hawaii State Energy Office. Richmond, CA: Geothermex Inc. Available at: <https://energy.hawaii.gov/wp-content/uploads/2011/10/Update-of-the-Statewide-Geothermal-Resource-Assessment-of-Hawaii.pdf> [Accessed 30 Oct. 2020].

Geothermex (2005). ASSESSMENT OF ENERGY RESERVES AND COSTS OF GEOTHERMAL RESOURCES IN HAWAII for THE STATE OF HAWAII DEPARTMENT OF BUSINESS, ECONOMIC DEVELOPMENT AND TOURISM. [online] Maui Tomorrow. Richmond, CA.: Geothermex Inc. Available at: <http://maui-tomorrow.org/pdf/geothermal-assessment-05.pdf> [Accessed 30 Oct. 2020].

Giambelluca, T., Chen, Q., Frazier, A., Price, J., Chen, Y.-L., Chu, P.-S., Eischeid, J., and Delparte, D., (2013). Online Rainfall Atlas of Hawai‘i. *Bull. Amer. Meteor. Soc.* 94, 313-316. 10.1175/BAMS-D-11-00228.1. doi.org/10.1175/BAMS-D-11-00228.1

Giambelluca, T., Shuai, X., Barnes, M., Alliss, R., Longman, R., Miura, T., Chen, Q., Frazier, A., Mudd, R., Cuo, L., and Businger, A., (2014). Evapotranspiration of Hawai‘i. Final report submitted to the U.S. Army Corps of Engineers—Honolulu District, and the Commission on Water Resource Management, State of Hawai‘i. <http://evapotranspiration.geography.hawaii.edu/downloads.html>

Graham, D. (2002). Noble Gas Isotope Geochemistry of Mid-Ocean Ridge and Ocean Island Basalts: Characterization of Mantle Source Reservoirs. *Reviews in Mineralogy and Geochemistry*, 47(1), pp.247–317. doi.org/10.2138/rmg.2002.47.8

Graham, D., Reid, M., Jordan, B., Grunder, A., Leeman, W. and Lupton, J. (2009). Mantle source provinces beneath the Northwestern USA delimited by helium isotopes in young basalts. *Journal of Volcanology and Geothermal Research*, 188(1–3), pp.128–140. doi.org/10.1016/j.jvolgeores.2008.12.004

Harðardóttir, S., Halldórsson, S. and Hilton, D. (2018). Spatial distribution of helium isotopes in Icelandic geothermal fluids and volcanic materials with implications for location, upwelling and evolution of the Icelandic mantle plume. *Chemical Geology*, 480, pp.12–27. doi.org/10.1016/j.chemgeo.2017.05.012

Hart, S., Blusztajn, J., Dick, H., Meyer, P. and Muehlenbachs, K. (1999). The fingerprint of seawater circulation in a 500-meter section of ocean crust gabbros. *Geochimica et Cosmochimica Acta*, 63(23–24), pp.4059–4080. doi.org/10.1016/S0016-7037(99)00309-9

- Hilton, D., Grönvold, K., O’Nions, R. and Oxburgh, E. (1990). Regional distribution of  $^3\text{He}$  anomalies in the Icelandic crust. *Chemical Geology*, 88(1–2), pp.53–67. doi.org/10.1016/0009-2541(90)90103-E
- Hilton, D., McMurtry, G. and Kreulen, R. (1997). Evidence for extensive degassing of the Hawaiian Mantle Plume from helium-carbon relationships at Kilauea Volcano. *Geophysical Research Letters*, 24(23), pp.3065–3068. doi.org/10.1029/97GL03046
- Hofmann, A., Farnetani, C., Spiegelman, M. and Class, C. (2011). Displaced helium and carbon in the Hawaiian plume. *Earth and Planetary Science Letters*, 312(1–2), pp.226–236. doi.org/10.1016/j.epsl.2011.09.041
- Holcomb, R., Reiners, P., Nelson, B. and Sawyer, N. (1997). Evidence for two shield volcanoes exposed on the island of Kauai, Hawaii. *Geology*, 25(9), pp.811–814. doi.org/10.1130/0091-7613(1997)025%3C0811:EFTSVE%3E2.3.CO;2
- Hunt, A., 2015, Noble Gas Laboratory’s standard operating procedures for the measurement of dissolved gas in water samples: U.S. Geological Survey Techniques and Methods, book 5, chap. A11, 22 p. dx.doi.org/10.3133/tm5A11
- Peek, S., Hurwitz, S., Elias, T., Nadeau, and Hunt, A, 2020, Helium isotopes and gas chemistry at Sulphur Banks, Kīlauea Volcano, Hawai‘i: U.S. Geological Survey data release, *in process*
- Ito, G., Frazer, N., Lautze, N., Thomas, D., Hinz, N., Waller, D., Whittier, R. and Wallin, E. (2017). Play fairway analysis of geothermal resources across the state of Hawaii: 2. Resource probability mapping. *Geothermics*, 70, pp.393–405. doi.org/10.1016/j.geothermics.2016.11.004
- Izuka, S. and Gingerich, S. (1997). Construction, geologic log and aquifer tests of the northeast Kilohana monitor well (State well 2-0124-01), Lihue, Kauai, Hawaii. USGS Open-File Report, (97–37). doi.org/10.3133/ofr9737
- Jackson, M.G., Konter, J.G. and Becker, T.W. (2017). Primordial helium entrained by the hottest mantle plumes. *Nature*, 542, pp.340–343. doi.org/10.1038/nature21023
- Kaufman, S. and Libby, W. (1954). The Natural Distribution of Tritium. *Physical Review*, 93(6), pp.1337–1344. doi.org/10.1103/PhysRev.93.1337
- Kelley, K., Plank, T., Ludden, J. and Staudigel, H. (2003). Composition of altered oceanic crust at ODP Sites 801 and 1149. *Geochemistry, Geophysics, Geosystems*, 4(6). doi.org/10.1029/2002GC000435
- Kelly, J. and Glenn, C. (2015). Chlorofluorocarbon apparent ages of groundwaters from west Hawaii, USA. *Journal of Hydrology*, 527, pp.355–366. doi.org/10.1016/j.jhydrol.2015.04.069
- Kennedy, B. (1988). Noble gases in vent water from the Juan de Fuca Ridge. *Geochimica et Cosmochimica Acta*, 52(7), pp.1929–1935. doi.org/10.1016/0016-7037(88)90016-6
- Kennedy, B. and van Soest, M. (2006). A helium isotope perspective on the Dixie Valley, Nevada, hydrothermal system. *Geothermics*, 35(1), pp.26–43. doi.org/10.1016/j.geothermics.2005.09.004

- Kennedy, K. (1985). Dikewater Relationships to Potential Geothermal Resources on Leeward West Maui, State of Hawaii (Master's thesis).  
[http://scholarspace.manoa.hawaii.edu/bitstream/handle/10125/21688/2100\\_r.pdf](http://scholarspace.manoa.hawaii.edu/bitstream/handle/10125/21688/2100_r.pdf)
- Kurz, M., Jenkins, W., Hart, S. and Clague, D. (1983). Helium isotopic variations in volcanic rocks from Loihi Seamount and the Island of Hawaii. *Earth and Planetary Science Letters*, 66, pp.388–406. doi.org/10.1016/0012-821X(83)90154-1
- Kurz, M. and Kammer, D. (1991). Isotopic evolution of Mauna Loa volcano. *Earth and Planetary Science Letters*, 103(1–4), pp.257–269. doi.org/10.1016/0012-821X(91)90165-E
- Larsen, E. and Gottfried, D. (1960). Uranium and Thorium In Selected Suites of Igneous Rocks. *American Journal of Science*, 258-A.
- Lau, L. and Hailu, T. (1968). Tritium measurements in natural Hawaiian waters: instrumentation. Honolulu (HI): Water Resources Research Center, University of Hawaii at Manoa. WRRRC technical report, 22. <https://scholarspace.manoa.hawaii.edu/handle/10125/7602>
- Lau L., and Hufen T., (1973). Tritium measurement of natural waters on Oahu, Hawaii: A preliminary interpretation (sampling period July 1969 to June 1970). Honolulu (HI): Water Resources Research Center, University of Hawaii at Manoa. WRRRC technical report, 65. <https://scholarspace.manoa.hawaii.edu/handle/10125/18100>
- Lautze, N., Thomas, D., Hinz, N., Apuzen-Ito, G., Frazer, N. and Waller, D. (2017). Play fairway analysis of geothermal resources across the State of Hawaii: 1. Geological, geophysical, and geochemical datasets. *Geothermics*, 70, pp.376–392. doi.org/10.1016/j.geothermics.2017.02.001
- Lautze, N., Thomas, D., Waller, D., Frazer, N., Hinz, N. and Apuzen-Ito, G. (2017b). Play fairway analysis of geothermal resources across the state of Hawaii: 3. Use of development viability criterion to prioritize future exploration targets. *Geothermics*, 70, pp.406–413. doi.org/10.1016/j.geothermics.2017.07.005
- Lautze, N., Ito, G., Thomas, D., Frazer, N., Martel, S.J., Hinz, N., Tachera, D., Hill, G., Pierce, H.A., Wannamaker, P.E. and Martin, T. (2020). Play Fairway analysis of geothermal resources across the State of Hawai'i: 4. Updates with new groundwater chemistry, subsurface stress analysis, and focused geophysical surveys. *Geothermics*, 86. doi.org/10.1016/j.geothermics.2019.101798
- Macdonald, G., Abbott, A. and Peterson, F., (1986). *Volcanoes In The Sea*. Honolulu: University of Hawaii Press.
- Martin, T., Brockhoff, C. and Creed, J. (1999).
- Matsumoto, T., Solomon, D., Araguás-Araguás, L. and Aggarwal, P., (2017). The IAEA's Coordinated Research Project on "Estimation of Groundwater Recharge and Discharge by Using the Tritium, Helium-3 Dating Technique": In Lieu of a Preface. *GEOCHEMICAL JOURNAL*, 51(5), pp.385-390. doi.org/10.2343/geochemj.2.0500
- McKinney, C., McCrea, J., Epstein, S., Allen, H. and Urey, H. (1950). Improvements in mass spectrometers for the measurement of small differences in isotope abundance ratios. *Rev. Sci. Instrum.* 21 (724). dx.doi.org/10.1063/1.1745698

- Méjean, P., Pinti, D., Kagoshima, T., Roulleau, E., Demarets, L., Poirier, A., Takahata, N., Sano, Y. and Larocque, M., (2020). Mantle helium in Southern Quebec groundwater: A possible fossil record of the New England hotspot. *Earth and Planetary Science Letters*, 545, p.116352. doi.org/10.1016/j.epsl.2020.116352
- Morgan, J., Park, J. and Zelt, C., (2010). Rift zone abandonment and reconfiguration in Hawaii: Mauna Loa's Ninole rift zone. *Geology*, 38(5), pp.471-474. doi.org/10.1130/G30626.1
- Müller, R., Sdrolias, M., Gaina, C. and Roest, W., (2008). Age, spreading rates, and spreading asymmetry of the world's ocean crust. *Geochemistry, Geophysics, Geosystems*, 9(4). doi:10.1029/2007GC001743
- McDougall, I., (1979). Age of shield-building volcanism of Kauai and linear migration of volcanism in the Hawaiian island chain. *Earth and Planetary Science Letters*, 46(1), pp.31-42. doi.org/10.1016/0012-821X(79)90063-3
- Neal, C., Brantley, S., Antolik, L., Babb, J., Burgess, M., Calles, K., Cappos, M., Chang, J., Conway, S., Desmither, L., Dotray, P., Elias, T., Fukunaga, P., Fuke, S., Johanson, I., Kamibayashi, K., Kauahikaua, J., Lee, R., Pekalib, S., Miklius, A., Million, W., Moniz, C., Nadeau, P., Okubo, P., Parcheta, C., Patrick, M., Shiro, B., Swanson, D., Tollett, W., Trusdell, F., Younger, E., Zoeller, M., Montgomery-Brown, E., Anderson, K., Poland, M., Ball, J., Bard, J., Coombs, M., Dietterich, H., Kern, C., Thelen, W., Cervelli, P., Orr, T., Houghton, B., Gansecki, C., Hazlett, R., Lundgren, P., Diefenbach, A., Lerner, A., Waite, G., Kelly, P., Clor, L., Werner, C., Mulliken, K., Fisher, G. and Damby, D., (2018). The 2018 rift eruption and summit collapse of Kīlauea Volcano. *Science*, 363(6425), pp.367-374. doi.org/10.1126/science.aav7046
- Ozima, M. and Podosek, F., (2002). *Noble Gas Geochemistry*. Cambridge: Cambridge University Press.
- Porcelli, D., Ballentine, C. and Wieler, R., (2002). *Noble Gases In Geochemistry And Cosmochemistry*. Washington: Mineralogical Society of America.
- Reyes, A., (1990). Petrology of Philippine geothermal systems and the application of alteration mineralogy to their assessment. *Journal of Volcanology and Geothermal Research*, 43(1-4), pp.279-309. doi.org/10.1016/0377-0273(90)90057-M
- Ribe, N. and Christensen, U., (1999). The dynamical origin of Hawaiian volcanism. *Earth and Planetary Science Letters*, 171(4), pp.517-531. doi.org/10.1016/S0012-821X(99)00179-X
- Rimstidt, J. and Barnes, H., (1980). The kinetics of silica-water reactions. *Geochimica et Cosmochimica Acta*, 44(11), pp.1683-1699. doi.org/10.1016/0016-7037(80)90220-3
- Sano, Y., Takahata, N. and Seno, T., (2006). Geographical Distribution of  $3\text{He}/4\text{He}$  Ratios in the Chugoku District, Southwestern Japan. *Pure and Applied Geophysics*, 163(4), pp.745-757. doi.org/10.1007/s00024-006-0035-0
- Scholl, M., Ingebritsen, S., Janik, C. and Kauahikaua, J., (1995). An isotope hydrology study of the Kilauea volcano area, Hawaii. USGS Water Resources Investigations Report, (95-4213). doi.org/10.3133/wri954213

- Sedwick, P., McMurtry, G., Hilton, D. and Goff, F., (1994). Carbon dioxide and helium in hydrothermal fluids from Loihi Seamount, Hawaii, USA: Temporal variability and implications for the release of mantle volatiles. *Geochimica et Cosmochimica Acta*, 58(3), pp.1219-1227. doi.org/10.1016/0016-7037(94)90587-8
- Seyfried, W. and Mottl, M. (1982). Hydrothermal alteration of basalt by seawater under seawater-dominated conditions. *Geochimica et Cosmochimica Acta*, 46(6), pp.985–1002. doi.org/10.1016/0016-7037(82)90054-0
- Sherrod, D., Hagstrum, J., McGeehin, J., Champion, D. and Trusdell, F. (2006). Distribution, <sup>14</sup>C chronology, and paleomagnetism of latest Pleistocene and Holocene lava flows at Haleakalā volcano, Island of Maui, Hawai‘i: A revision of lava flow hazard zones. *Journal of Geophysical Research: Solid Earth*, 111(B5). doi.org/10.1029/2005JB003876
- Sherrod, D., Sinton, J., Watkins, S., and Brunt, K., (2007). Geologic map of the State of Hawai‘i: U.S. Geological Survey Open-File Report 2007-1089 [<http://pubs.usgs.gov/of/2007/1089/>].
- Simkin, T., Tilling, R., Vogt, P., Kirby, S., Kimberly, P., and Stewart, D., (2006). This dynamic planet; World Map of Volcanoes, Earthquakes, Impact Craters, and Plate Tectonics: U.S. Geological Survey Geologic Investigations Series Map I-2800.
- Simmons, S. and Brown, K. (2006). Gold in Magmatic Hydrothermal Solutions and the Rapid Formation of a Giant Ore Deposit. *Science*, 314(5797), pp.288–291. doi.org/10.1126/science.1132866
- Sisson, T. (2019). Temperatures and depths of Hawaiian magmas. [online] [www.mantleplumes.org](http://www.mantleplumes.org). Available at: [http://www.mantleplumes.org/HawaiiFocusGroup/Sisson\\_abs.html](http://www.mantleplumes.org/HawaiiFocusGroup/Sisson_abs.html) [Accessed 6 Nov. 2020].
- Smith, S. and Kennedy, B. (1983). The solubility of noble gases in water and in NaCl brine. *Geochimica et Cosmochimica Acta*, 47(3), pp.503–515. doi.org/10.1016/0016-7037(83)90273-9
- Sorey, M. and Colvard, E. (1994). Potential effects of the Hawaii Geothermal Project on ground-water resources on the island of Hawaii. U.S. Geologic Survey Water-Resources Investigations Report, 94–4028. doi.org/10.3133/wri944028
- Stanley, R., Baschek, B., Lott, D. and Jenkins, W. (2009). A new automated method for measuring noble gases and their isotopic ratios in water samples. *Geochemistry, Geophysics, Geosystems*, 10(5). doi.org/10.1029/2009GC002429
- Staudigel, H., Plank, T., White, B. and Schmincke, H. (2013). Geochemical Fluxes During Seafloor Alteration of the Basaltic Upper Oceanic Crust: DSDP Sites 417 and 418. *Geophysical Monograph Series*, pp.19–38. doi.org/10.1029/GM096p0019
- Sweeney, M. and Burtchard, G. (1995). Archaeology in the Kilauea East Rift Zone: Part 2, A preliminary sample survey, Kapoho, Kamaili and Kilauea geothermal subzones, Puna District, Hawaii island. U.S. Department of Energy Technical Report, ORNL/SUB-94-SN-150/2. doi.org/10.2172/210948

- Templeton, A. and Ellison, E. (2020). Formation and loss of metastable brucite: does Fe(II)-bearing brucite support microbial activity in serpentinizing ecosystems? *Philosophical Transactions of the Royal Society A: Mathematical, Physical and Engineering Sciences*, 378(2165), p.20180423. doi.org/10.1098/rsta.2018.0423
- Thomas, D.M., (1982). A Geochemical Case History of the HGP-A Well 1976-1982. Hawaii Institute of Geophysics Contribution No. 1293, pp. 6.
- Thomas, D. (1985). Geothermal resources assessment in Hawaii: final report. [online] scholarspace.manoa.hawaii.edu. Available at: <https://scholarspace.manoa.hawaii.edu/handle/10125/20125?mode=full> [Accessed 30 Oct. 2020].
- Thomas., D., Cox, M., Erlandson, D. and Kajiwar, L. (1979) Potential geothermal resources in Hawaii: a preliminary regional survey. Hawaii Inst. Geophys. Tech. Rept. HIG-79-4.
- Thomas, D., Cuff, K. and Cox, M. (1986). The association between ground gas radon variations and geologic activity in Hawaii. *Journal of Geophysical Research: Solid Earth*, 91(B12), pp.12186–12198. doi.org/10.1029/JB091iB12p12186Thomas et.al 1987
- Thomas, D., Paillet, F. and Conrad, M. (1996). Hydrogeology of the Hawaii Scientific Drilling Project borehole KP-1: 2. Groundwater geochemistry and regional flow patterns. *Journal of Geophysical Research: Solid Earth*, 101(B5), pp.11683–11694. doi.org/10.1029/95JB03845
- Torgersen, T. and Jenkins, W. (1982). Helium isotopes in geothermal systems: Iceland, The Geysers, Raft River and Steamboat Springs. *Geochimica et Cosmochimica Acta*, 46(5), pp.739–748. doi.org/10.1016/0016-7037(82)90025-4
- Tree, J. (2016). Mantle Potential Temperatures of 4.5 to 47 MA Hawaiian Volcanoes Using Olivine Thermometry: Implications for Melt Flux Variations. [online] scholarspace.manoa.hawaii.edu. Available at: <https://scholarspace.manoa.hawaii.edu/handle/10125/51579> [Accessed 7 Nov. 2020].
- Truesdell, A., Haizlip, J., Armannsson, H. and D'Amore, F. (1989). Origin and transport of chloride in superheated geothermal steam. *Geothermics*, 18(1–2), pp.295–304. doi.org/10.1016/0375-6505(89)90039-4
- University of Hawaii. (2015). Hawaii Play Fairway Analysis: Hawaii Water Well Temperature and Hydraulic Head [data set]. Retrieved from <https://dx.doi.org/10.15121/1254459>.
- Valbracht, P., Staudacher, T., Malahoff, A. and Allègre, C. (1997). Noble gas systematics of deep rift zone glasses from Loihi Seamount, Hawaii. *Earth and Planetary Science Letters*, 150(3–4), pp.399–411. doi.org/10.1016/S0012-821X(97)00094-0
- Watson, S. and McKenzie, D. (1991). Melt Generation by Plumes: A Study of Hawaiian Volcanism. *Journal of Petrology*, 32(3), pp.501–537. doi.org/10.1093/petrology/32.3.501
- Weiss, R.F. (1968). Piggyback sampler for dissolved gas studies on sealed water samples. *Deep Sea Research and Oceanographic Abstracts*, 15(6), pp.695–699. doi.org/10.1016/0011-7471(68)90082-x

Welhan, J., Poredai, R., Rison, W. and Craig, H. (1988). Helium isotopes in geothermal and volcanic gases of the western United States, I. Regional variability and magmatic origin. *Journal of Volcanology and Geothermal Research*, 34(3–4), pp.185–199. doi.org/10.1016/0377-0273(88)90032-7

West, H., Garcia, M., Gerlach, D. and Romano, J. (1992). Geochemistry of tholeiites from Lanai, Hawaii. *Contributions to Mineralogy and Petrology*, 112(4), pp.520–542.

Zierenberg, R., Shanks III, W., Seyfried Jr., W., Koski, R. and Strickler, M. (1988). Mineralization, alteration, and hydrothermal metamorphism of the ophiolite-hosted Turner-Albright sulfide deposit, southwestern Oregon. *Journal of Geophysical Research*, 93(B5), p.18.

Zurek, J., Williams-Jones, G., Trusdell, F. and Martin, S. (2015). The origin of Mauna Loa's Nīnole Hills: Evidence of rift zone reorganization. *Geophysical Research Letters*, 42(20), pp.8358–8366. doi.org/ 10.1002/2015gl065863